REPORT DOCUMENTATION PAGE

Form Approved OMB NO. 0704-0188

1. AGENCY USE ONLY (Leave Blank)	2. REPORT DATE:	3. REPORT TYPE AND DATES COVERED Final Report 25-Sep-2003 - 31-May-2006

4. TITLE AND SUBTITLE

Unsteady Storm Drainage Modeling Within the U.S. Army Corps of Engineers GSSHA Model

5. FUNDING NUMBERS

DAAD190310355

6. AUTHORS

Fred L. Ogden

8. PERFORMING ORGANIZATION REPORT NUMBER

7. PERFORMING ORGANIZATION NAMES AND ADDRESSES

University of Connecticut - Storrs
Office for Sponsored Programs
438 Whitney Rd. Ext., Unit 1133
Storrs, CT 06269 -1133

9. SPONSORING/MONITORING AGENCY NAME(S) AND ADDRESS(ES)

U.S. Army Research Office
P.O. Box 12211
Research Triangle Park, NC 27709-2211

10. SPONSORING / MONITORING AGENCY REPORT NUMBER

45797-EV.1

11. SUPPLEMENTARY NOTES

The views, opinions and/or findings contained in this report are those of the author(s) and should not contrued as an official Department of the Army position, policy or decision, unless so designated by other documentation.

12. DISTRIBUTION AVAILIBILITY STATEMENT

Approved for Public Release; Distribution Unlimited

12b. DISTRIBUTION CODE

13. ABSTRACT (Maximum 200 words)

The abstract is below since many authors do not follow the 200 word limit

14. SUBJECT TERMS

subsurface, tile drains, groundwater, surface-water, interactions, storm sewers

15. NUMBER OF PAGES

Unknown due to possible attachments

16. PRICE CODE

17. SECURITY CLASSIFICATION OF REPORT	18. SECURITY CLASSIFICATION ON THIS PAGE	19. SECURITY CLASSIFICATION OF ABSTRACT	20. LIMITATION OF ABSTRACT
UNCLASSIFIED	UNCLASSIFIED	UNCLASSIFIED	UL

NSN 7540-01-280-5500

Standard Form 298 (Rev .2-89)
Prescribed by ANSI Std.
239-18 298-102

Report Title

Unsteady Storm Drainage in the US Army Corps of Engineers, Engineering Research and Development Center, Gridded Surface/Subsurface Hydrologic Analysis (GSSHA) Model

ABSTRACT

The ability to specifically simulate unsteady hydraulics in subsurface storm and tile drains was included in the formulation of the Gridded Surface Subsurface Hydrologic Analysis (GSSHA) model. Simulations were performed to determine model sensitivity to parameters, and the hydrologic significance of subsurface drains.

List of papers submitted or published that acknowledge ARO support during this reporting period. List the papers, including journal references, in the following categories:

(a) Papers published in peer-reviewed journals (N/A for none)

Downer, C.W., F.L. Ogden, J.M. Niedzialek, and S. Liu, 2005, Gridded Surface/Subsurface Hydrologic Analysis (GSSHA) Model: A Model for Simulating Diverse Streamflow-Producing Processes, p 131-158, in Watershed Models, V.P. Singh, and D. K. Frevert, Eds., CRC Press, 680 pp.

Number of Papers published in peer-reviewed journals: 1.00

(b) Papers published in non-peer-reviewed journals or in conference proceedings (N/A for none)

Number of Papers published in non peer-reviewed journals: 0.00

(c) Presentations

Byrd, A., and G. Eggers, 2006, Surface Water/Groundwater Interaction Improvements to GSSHA, Joint Eighth Federal Interagency Conference and Third Federal Interagency Hydrologic Modeling Conference, April 2-6, Silver Legacy, Hotel, Reno, Nevada.

Dilaj, D., and F.L. Ogden, 2005, Testing of hydrologic importance of tile drain formulation in GSSHA, Presentation to U.S. Army Corps of Engineers, Engineering Research and Development Center, Coastal and Hydraulics Laboratory, Vicksburg, Mississippi, GSSHA workshop, 26 July.

Number of Presentations: 2.00

Non Peer-Reviewed Conference Proceeding publications (other than abstracts):

Number of Non Peer-Reviewed Conference Proceeding publications (other than abstracts): 0

Peer-Reviewed Conference Proceeding publications (other than abstracts):

Ogden, F.L., and J.M. Niedzielek, 2003, Physics-Based Distributed Rainfall-Runoff Modeling of Urbanized Watersheds Revisited with GSSHA,
World Water and Environmental Resources Congress 2003, ASCE/EWRI, Paul Bizier, Paul DeBarry - Editors, June 23–26, 2003, Philadelphia, Pennsylvania, USA.

Number of Peer-Reviewed Conference Proceeding publications (other than abstracts): 1

(d) Manuscripts

Ogden, F. L., Niedzialek, J. M., and Byrd, A. R. (2005b). “Storm drain effects on urban flooding,” SWWRP Technical Notes Collection, In preparation, U.S. Army Engineer Research and Development Center, Vicksburg, MS. https://swwrp.usace.army.mil/ (under review)

Number of Manuscripts: 1.00

Number of Inventions:

Graduate Students

NAME	PERCENT_SUPPORTED	
Jon Zahner, M.S.	0.25	No
Derek Dilaj, M.S.	0.25	No
Justin Niedzialek, Ph.D.	0.13	No
FTE Equivalent:	**0.63**	
Total Number:	**3**	

Names of Post Doctorates

NAME	PERCENT_SUPPORTED	
Siqing Liu	0.13	No
FTE Equivalent:	**0.13**	
Total Number:	**1**	

Names of Faculty Supported

NAME	PERCENT_SUPPORTED	National Academy Member
Fred L. Ogden	0.09	No
FTE Equivalent:	**0.09**	
Total Number:	**1**	

Names of Under Graduate students supported

NAME	PERCENT_SUPPORTED
FTE Equivalent:	
Total Number:	

Names of Personnel receiving masters degrees

NAME	
Jon A. Zahner	No
Total Number:	**1**

Names of personnel receiving PHDs

NAME
Total Number:

Names of other research staff

NAME	PERCENT_SUPPORTED
FTE Equivalent:	
Total Number:	

Sub Contractors (DD882)

Inventions (DD882)

Influence of Storm Sewers, Drainage Density, and Soil Moisture On Runoff From an Urbanizing Catchment

Jonathan A. Zahner

B.S., University of Connecticut, 2002

A Thesis
Submitted in Partial Fulfillment of the
Requirements for the Degree of
Master of Science
at the
University of Connecticut
2004

APPROVAL PAGE

Master of Science Thesis

Influence of Storm Sewers, Drainage Density, and Soil Moisture
On Runoff From an Urbanizing Catchment

Presented by

Jonathan A. Zahner, B.S.

Major Advisor _____
Fred L. Ogden

Associate Advisor _____
Amvrossios C. Bagtzoglou

Associate Advisor _____
Glenn S. Warner

University of Connecticut

2004

ACKNOWLEDGMENTS

The author would like to express thanks to all who contributed to this research. Dr. Zhong Ji, the creator of the SUPERLINK algorithm, answered questions with patience regarding his paper on the scheme. Dr. Ji also corrected typographical errors in his publication and discussed changes to his original approach by the author.

The research team at Princeton University under the supervision of Dr. James Smith provided most of the data for the Dead Run watershed and Hurricane Isabel. Katherine Meirediercks assisted in the storm drainage network data collection and assimilation process, as well as stream flow and precipitation data.

The University of Connecticut Watershed Modeling Group was instrumental in all phases of this research. Dr. Fred Ogden, advisor to the author, offered an abundance of hydrologic modeling advice. Dr. Ogden also assisted in data analysis and was the principal reviewer of this thesis. Justin Niedzialek provided expertise in model setup in WMS and GSSHA. Michael Rogalus III lent support with GIS data manipulation.

The following grants funded the author on this research:

National Science Foundation Grant EAR-0003408

U.S. Army Research Office Grant DAAD19-03-1-0355

TABLE OF CONTENTS

LIST OF FIGURES

ABSTRACT

A study was undertaken to examine the influence of manmade changes to the drainage network on flooding from urbanized catchments. The literature contains contradictory hypotheses regarding the influence of different structural changes. Testing of these hypotheses is facilitated by the use of a physics based hydrologic model. A distributed physically based hydrologic model Gridded Surface Subsurface Hydrologic Analysis (GSSHA) was combined with SUPERLINK, a storm drainage scheme. Factors that were tested include storm drainage networks, impervious areas, drainage density, width function, and initial soil moisture. Results indicate that the subsurface drainage network is important for moderate rainfall events, but largely overwhelmed for extreme events. Flood magnitude increases due to modifications to the channel network are dominant compared to effects from impervious area. Initial soil moisture likewise impacts moderate storms, but its importance diminishes during extreme events.

I. INTRODUCTION

There is no argument that flood magnitude and frequency increase as urban development spreads throughout a watershed. It is obvious that understanding this trend is of great social and economic importance. But what causes this change in hydrology is the source of much debate and numerous studies. The hydrologic processes affected by urbanization are primarily infiltration and surface runoff. Comparisons between basins of varying land use and drainage systems can provide some insight into what feature plays the dominant role. However, it is impossible to eliminate differences in scale, topography, geometry, and geology in such multi-basin analyses. A numerical model stands out as the best method to systematically isolate watershed properties that affect its hydrologic response.

Distributed-parameter models are gaining a foothold in the world of hydrologic modeling, as these methods are capable of describing spatially varied land-surface modifications. A major deficiency of most these models, however, is their inability to explicitly handle storm drainage networks. The purpose of this thesis was twofold: to integrate a unique storm drainage algorithm to an existing distributed hydrologic model, and to test hypotheses using data from a watershed where urbanizing drainage effects are considerable. This study consists of five primary hypotheses relating to: the storm drainage network, impervious areas, drainage density, the distribution of drainage within a watershed, and pre-storm soil moisture.

Changes in urban runoff volume and flood peaks have historically been blamed on increases in impervious area. This theory was recently challenged by a study in and around Charlotte, North Carolina (Smith et al. 2002). The essence of their conclusions

was that the increase in storm drainage connectivity and hence hydraulic efficiency played the greatest role in increasing flood magnitudes. They also concluded that antecedent soil moisture and drainage density distribution within the watershed play an important role in flooding.

Storm sewers enhance the drainage efficiency of a watershed, but their impact compared to other modifications is unknown. The model developed here provides a unique and powerful tool for assessing hydrology in an urban catchment. Storm sewers are often overwhelmed during extreme events, so it is possible that their effect diminishes as the precipitation intensity increases.

Simulations are also performed with different combinations of impervious area and drainage network densities. Analysis of these results identify which watershed feature is more influential in increasing flood magnitudes. Understanding the role of impervious coverage versus storm sewers could be useful in guiding the storm water management practices of urbanizing areas, as well as solutions to flooding in urban environments.

Drainage density represents the length of stream channels in a basin relative to total drainage area. A sensitivity analysis on this parameter might show the range of drainage densities that have the strongest effect on flood peaks. This dimensionless measurement may be useful to predict the effect of development on other watersheds. Similarly, the spatial distribution of the drainage network is tested for its influence on basin response. This distribution is measured by a statistical parameter known as the width function. Relating the width function to flood peaks likewise might provide generalized conclusions about the location of drainage within a watershed.

Soil moisture preceeding an event can have a significant impact on the runoff generating mechanisms. Simulating a watershed with all properties being identical except initial soil saturation points to the importance of this soil parameter. A greater understanding of the role of antecedent soil moisture could improve flood prediction accuracy. A coupled surface-storm sewer model has the potential to explore each of these hydrologic processes, and provide conclusions of scientific and practical impact.

The specific objectives of this thesis are to:

1) Implement a sophisticated storm network model and couple it with a distributed hydrologic model
2) Explore the importance of engineered subsurface storm drainage networks
3) Evaluate the role of impervious areas
4) Compare the effect of varying degrees of drainage density
5) Determine the role of the width function in watershed runoff
6) Evaluate the role of initial soil moisture in urban basins.

II. BACKGROUND

Literature Review

Analysis of the effects of urbanization on watershed hydrology is not new. Studies dating back to the late 1800's have been concerned with flooding in settings such as urban England. It is therefore critical to become familiar with previous attempts to understand the nature of storm drainage systems and their effect on flooding, as well as general changes in land use. The availability of computing power has revolutionized techniques of hydrologic modeling, and thus our understanding of the processes has improved.

There is no question that land surface modifications related to urban development have increased the magnitude and frequency of flooding around the globe. Each of the research efforts included in the following review cites the importance of understanding the nature of anthropogenic effects on a catchment's drainage characteristics. These observed changes in stream flow have been modeled with empirical techniques largely dependent on assumptions of the controlling factors of urban runoff. Indeed, the commonly accepted principal variable for much of the 20th century has been the extent of impervious area. Leopold (1968) presented an empirical analysis of impervious coverage that became a benchmark of urban watershed theory. Essentially, this research showed that increases in impervious area were accompanied by elevated flood peaks and a decrease in inter-storm flows. Although Leopold acknowledged the concept that storm sewers decrease the lag time, the drainage network was given a secondary role to land use. Leopold compiled a table based on contemporary research of Carter (1961), Anderson (1968) and others. By providing two values, percentage impervious and

percentage sewered, one could estimate the increase in flood peaks. Based upon this theory, simplifying assumptions have been made in urban hydrologic modeling. Primarily, it has been assumed that the effect of urbanization can be described by the fraction of impervious area. Secondly, it is commonly thought that large-scale events will overwhelm a storm drainage system, and thus their total contribution to runoff is small.

Climate

Many studies have focused on other reasons for increasing flood magnitudes and frequencies. Some have pointed to changing climate, including work by Reynard et al. (2001). These studies mainly pertain to large catchments on the order of 10,000 sq km, and are far too coarse to describe the small-scale effects of urbanization. Howe and White (2000) refuted the claim that global warming is to blame for increased urban flooding. From a political policy standpoint, they criticized the practice of straightening rivers and expanding local drainage systems. This common solution to localized flooding concerns simply moves the problem downstream, as both time to peak and attenuation are decreased. They note that there must be a comprehensive plan that incorporates all scales of drainage in order to reverse the current trend of flooding. Their suggestions include constructing wetlands to recreate the original flow attenuation.

Land Use

Land use changes have been the focus of many flood related studies. Beighley and Moglen (2003) attempted to compare flood peaks from pre-urbanized flow records to

current urbanized flow data. For example, they postulate that a 100 year flood in the 1950's would be a 75 yr flood in the 1990's. Their method of correcting flows to represent statistically similar floods was applied to current watershed conditions. They focused on three factors: increases in urban land use, decreases in forested land, and the percent overall urbanization classified as "high density development". It was found that none of these land use factors were effective for estimating the adjusted flood flows. Surprisingly, a spatial parameter describing the location in the basin in which development occurred could best predict the adjusted flows. Development occurring farthest from the basin outlet had the greatest effect on peak flows, and thus they noted the need to investigate changes in channel roughness. The use of a detailed hydrologic model could explore both the land use question and spatial observation. Crooks and Davies (2001) presented additional research on the issue of land use. Using 30 years of data of land use change and its flooding effects in the Thames, England catchment, they found that coverage had an insignificant role compared to rainfall at a large scale. These findings point to the fact that another process dominates flood dynamics in an urbanizing watershed.

Channel & Drainage Network Morphology

Research into the role of drainage networks in flooding is not new. Some of the earliest work was done by Anderson (1970) on the effects of urban development on floods in northern Virginia. He gathered rainfall and runoff data on 81 similar watersheds, developed relationships between size, length, slope, percent impervious, and type of drainage system. Using a comparative approach between basins with one or more

similar characteristics, Anderson predicted the effect of changing one variable. Drainage system improvements were shown to reduce the lag time of a flood by up to 12%. The same lag time was predicted for a sewered system with impervious areas versus pervious surfaces, but with a higher magnitude flood. Regardless of land surface changes, the effect of sewer installation was to increase the flood peak magnitude by a factor of 2 or 3 for smaller events. While a completely impervious surface could increase the flood magnitude by 2.5 times, the effect of this land surface condition decreased as the storm total rainfall grew. In fact, he predicted that the land surface modifications in some catchments were negligible for a 100-year flood, as the entire watershed would behave as impervious. Though these results were based on estimates and empirical relationships, the conclusions certainly opened the way for new drainage network studies.

In more recent channel research, Wolff and Burges (1994) used the model DAMBRK to explore the effects of river channel properties on downstream flood frequency. They concluded that an increase in storage in the channels decreases the flood peaks. An interesting possibility elucidated by Wolff and Burges (1994) is that alternatively, covered channels (culverts) decrease the storage capacity, forcing excess flow to the overland plain, elevating local flooding.

Despite the focus of this study on urban and developing watersheds, research on an undeveloped watershed by Troch et al. (1994) introduced relevant findings related to flow velocities. Using empirical and model-based analysis from a small catchment in the Appalachians, they sought to draw a connection between peak discharge times and flow velocities. For lower overland flow velocities (due to high roughness values), the channel velocity did not influence flood peak timing. However, as overland roughness

decreased, the channel properties began to control lag times. Below a critical overland roughness value, time to peak was completely governed by channel roughness. Although this critical overland roughness threshold was below a naturally occurring value, the study suggests that urban land covers with low roughness (i.e. rooftops and parking lots) transfer control of lag time from the overland plain to the channel properties.

Related modeling

Much of this review has been of conceptual and regional scale studies. Since the focus of this research is on small scale distributed hydrologic modeling, a review of similar modeling efforts is relevant. A comparable approach to storm drainage modeling was found in the literature by Hsu et al. (2000). A heavy typhoon was simulated over a catchment subject to flooding in Taipei, Taiwan. Much of the city is protected by levees and thus dependant on pump stations to remove storm water. The focus of their study was on areas of inundation, not considering the effect of the drainage network on lag time and flood magnitudes. Using the storm sewer module of SWMM and a two-dimensional diffusive wave overland flow routine, the authors showed that the storm drains increased the areas of ponded water. Linkage of the two models was not well explained, but it appeared that the models were not run simultaneously. In a situation where flooded network discharge back onto the overland plain is a consideration, it is critical that the model components simulate the hydrologic processes in parallel.

Additional modeling to assess the causes of increasing flood peaks near Charlotte, North Carolina Turner-Gillespie et al. (2003) focused on attenuating reaches. In this study, floodplain roughness was tested for its control over flood peaks and lag timing.

Although decreasing roughness in overland flow associated with urbanization did produce higher peaks and quicker lag times, the relative effect was small. However, it was found that watershed scale flood peaks were very sensitive to the tributary response time. This same conclusion could likely be drawn for storm drainage networks, which generally replace natural tributaries.

Width function

An investigation into the nature of urbanizing stream networks by Graf (1977) showed a drastic increase in the number, length, and density of man-made channels in an Iowa catchment with extensive historical data. Though he did not specifically address subterranean conduits, the research on artificially altered streams is still applicable. Statistical analysis with power law equations showed a high sensitivity of time to peak and kurtosis (peakedness) for channel modifications.

The density of links in a drainage network mentioned by Graf (1977) can be described by a statistic now known as the width function. Generally, the width function is defined as a plot of the number of channel segments at a specified distance from the basin outlet (Rodriguez-Iturbe and Rinaldo, 1997). Attempts have been made to relate the width function to peak discharges, including work by Veitzer and Gupta (2001). Focusing strictly on network properties, they determined that the width function alone does not provide enough to formulate a substantial connection between drainage structure and flow peaks. It is clear that additional information is necessary for the width function to be useful. A slightly different approach defines the width function as the drainage area at a flow distance from the outlet (Richards-Pecou, 2002). Although their particular

study assumed a constant flow velocity in the channels, this work showed increasing peaks as the width function was elevated over natural conditions.

An excellent example using the width function concept was performed by Smith et al. (2002) who studied the heavily urbanized Charlotte, North Carolina basin. Five of the largest flood peaks in a 74 year record had occurred within the last 6 years of record on the Little Sugar Creek catchment. In an attempt to relate the extensive urban and suburban growth since 1960 to the increased flooding, their research examines hydrometeorology, soil moisture, impervious area, and drainage network modification. The methodology concentrates on diagnostic testing of each large event, as the target was regional hydrology. However, their findings provide hypotheses for our study. A detailed physical model can be used to investigate the relative effect of these hydrologic and hydraulic elements.

Changes in landuse have traditionally been blamed for flooding, but surprisingly did not play a major role in overall water balance for the five extreme events. The most important landuse type, impervious area, did correlate to flood peak timing and magnitude. However, the extreme events of interest consist of rainfall rates far higher than saturated hydraulic conductivity values. Thus infiltration excess is the dominant runoff mechanism with or without the impervious coverage. Antecedent soil moisture was shown to play an important role for some events, as dry soil conditions consumed an appreciable amount of water through infiltration.

Of greatest interest is their conclusion that expansion of the drainage network played a central role in the rising trend of flood peaks. A distinct alteration in width function could be seen in the lower section of Little Sugar Creek, having the effect of

decreasing lag time and increasing flood magnitudes. Attenuating reaches were shown to have significant impact on reducing peak discharge, and conversely channelizing these reaches would have the opposite effect.

Storm Drainage Model Selection

GSSHA

The need to simulate surface water flows in watersheds with diverse runoff production mechanisms has prompted the development of a physically based hydrologic model, called the Gridded Surface/Subsurface Hydrologic Analysis (GSSHA) model (Downer and Ogden, 2004). GSSHA simulates stream flow generated by both infiltration excess and saturation excess mechanisms. The model employs mass-conserving solutions of partial differential equations and closely links the hydrologic components to assure an overall mass balance. It is not, however, capable of modeling storm sewers. A sub-model within the GSSHA framework to directly handle subterranean sewers and grate inlets would allow modeling of complex urban catchments. The concept of numerical storm water modeling is not new, and thus the selection of a modeling approach required review of existing methods. This review includes commonly available models as well as some lesser-known methods, and a short description of each.

USGS Full Equations model (FEQ)

The FEQ model (USGS, 1997) has been shown to accurately model free surface flow using a four point implicit Preissmann scheme. For conduits flowing full, the free surface assumption disappears. This problem is commonly avoided by the implementation of a "Preissmann slot", a narrow slot extending from the top of the pipe in which flow is permitted. The weakness of this model is that the slot is assumed never to be overtopped, thus preventing surcharged manholes or flow back into the overland plain. Additionally, Meselhe and Holly (1997) demonstrated that for Froude numbers

near 1.0, the Preissmann 4 point scheme is unstable. This creates problems where bed slopes change rapidly and other trans-critical flow situations as well as free jet outlet conditions. Given these limitations, the FEQ model was not found suitable for general storm sewer modeling.

U.S. National Weather Service DWOPER

The Dynamic Wave OPERational (DWOPER) model, developed by Fread (1976), solves the conservation of mass and conservation of energy equations. This one dimensional, unsteady flow model allows for wave propagation in the upstream and downstream direction to account for situations of hurricane surge and complex backwater effects. DWOPER is limited in cross section interpolation and its inability to model supercritical flow (NWS, 2003).

SWMM

Development of the U.S. Environmental Protection Agency's Storm Water Management Model (SWMM) began in the late 60's, and has since undergone many improvements. The model contains four distinct modules, Runoff, Transport, Extran, and Storage/Treatment. The Extran module was of interest to this review, as it allows for pipe flow with backwater, surcharge, pressurized flow, and looped networks. Solving the de St-Venant equations explicitly is a noted weakness, as it tends to become unstable at long time steps and is computationally inefficient. Because the existing code is a product of 30 years of development, it would be difficult to merge a specific component to suit the needs of this research (USEPA, 2002). Although the planned overhaul of SWMM

would make it more adaptable to other applications, there are components of the model such as the land surface parameterization scheme that cannot match the sophistication of GSSHA.

Danish Hydraulics Institute MOUSE

The MOUSE pipeflow model accounts for all of the critical elements of a storm drainage model including flow reversal, backwater effects, pressurized flow, surcharged manholes, and storage basins. It solves the full-dynamic form of the de St. Venant equations by an implicit, finite difference formulation with an adaptive time step. However, a thorough analysis of the techniques employed in MOUSE is impossible. The source code is not available since MOUSE is proprietary software, making re-development too complex.

SUPERLINK Scheme

The SUPERLINK model, developed by Ji (1998), is a general hydrodynamic model for sewer/channel networks. This method solves the full dynamic de St. Venant equations in one dimension and employs the Preissman Slot to extend the open channel flow assumptions to closed conduits flowing full and surcharged. Unlike many applications of the Preissman slot, SUPERLINK does not consider the area of the narrow slot in the flow calculations or wetted perimeter, thus reducing the error associated with this concept. Another significant benefit of this model is its staggered grid implicit solution to the full equations of motion, enhancing stability and computational speed.

Of these schemes, SUPERLINK was judged the most capable with a very detailed description of the formulation allowing implementation. Although it has not had the widespread use and acceptance as many of the other models, Ji (1998) tested this scheme on a complex data set from the city of Winnipeg, Manitoba, Canada. Winnipeg, located on the banks of the Red River, is a very low gradient watershed (subject to backwater effects and surcharging) and contains multiple looped and branched pipes. Ji compared SUPERLINK output to both SWMM Extran and physical observations, with favorable results against both. SUPERLINK was stable at a 400 second time step, compared to a 7 second Extran time step, and generated mass conservation errors of only 0.32% over a 5-hour simulation period. Based on the comprehensive formulation and satisfactory simulation results, SUPERLINK was chosen as the pipe network model to couple with GSSHA.

III. PIPE NETWORK DEVELOPMENT & TESTING

SUPERLINK Review

Network Nomenclature

To understand the following discussion, it is important to review the network definitions and rules. *Superlinks* are series of links connecting junctions, and must have a junction on either end. A *junction* is defined as a point where two or more superlinks meet, or the unconnected end of a superlink (such as intake/discharge point of network). A *link* is a segment of a superlink connecting two nodes, and a *node* is a computational point in a superlink. Nodes exist adjacent to both upstream and downsteam junctions of a superlink, thus the number of nodes is equal to one plus the number of links.

Each *junction* is assigned a number, 1 through number of junctions, generally ordered from top of catchment down. Each superlink is assigned a number, 1 through number of superlinks, in general order from top of catchment down. Within a superlink, *node* numbering starts at the first upstream node (adjacent to upstream junction) and continues through number of links plus 1. A *link* has the same index as its upstream node, 1 through number of links. The nature of drainage networks often includes looped systems, and thus the numbering scheme must be capable of representing this. Although the algorithm is not limited by the order in which components are labeled, computational efficiency is gained through organized numbering. For model stability and accuracy, a minimum number of 3 links (4 nodes) are required for each superlink.

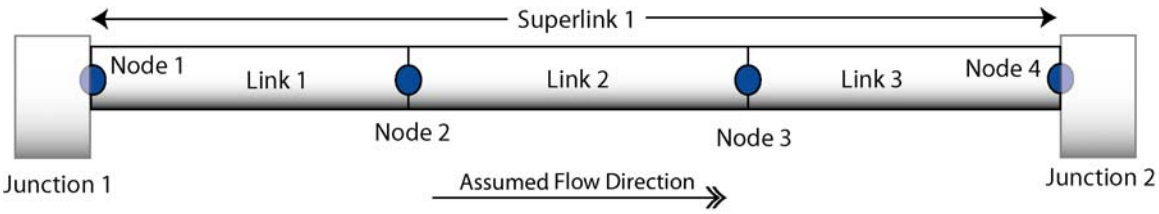

Figure 1 SUPERLINK junction, link, and node nomenclature

Inflow is allowed at junctions and nodes via two primary structures. The first is a culvert, which captures a natural stream channel, and only is possible at a junction. The second is any type of grate/curb opening in a roadway, and is possible at either a junction or a node. Discharge can occur from either a flooded manhole, drop inlet, or an outlet pipe (node or junction), and junctions may discharge directly into a channel. The parameters for these inlets and outlets are contained in the node and junction cards defined in the file format.

The use of both nodes and links may seem redundant, but in fact is quite integral to the "staggered grid" technique employed in SUPERLINK. There are two variables that must be solved throughout the system at each time step: depth and flow. In this approach, depth and flow are considered at two distinct locations; depth is computed at nodes, and flow in links. Calculating these two variables at the same point is a source of instability because they are not independent. SUPERLINK is capable of modeling long time steps due to this staggered feature coupled with the implicit solution to be discussed.

Modeling Theory

The basic concepts of the SUPERLINK scheme have been briefly outlined. Here, the theory behind the algorithm will be explored further. The central equations solved in

this model are the conservation of mass (1) and the de St. Venant equation of motion (2). This pair of nonlinear partial differential equations take the form of:

$$\frac{\partial A}{\partial t} + \frac{\partial Q}{\partial x} = q_0 \qquad (1)$$

$$\frac{\partial Q}{\partial t} + \frac{\partial Qu}{\partial x} + gA\left(\frac{\partial h}{\partial x} - S_0 + S_f + S_L\right) = 0 \qquad (2)$$

where A = flow cross-sectional area, Q = discharge, h = depth, u = velocity, S_0 = bed slope of conduit, S_f = friction head loss slope, S_L = local head loss slope, q_0 = lateral flow to conduit, g = gravitational constant, x = distance, and t = time.

The two central equations (1 & 2) are applied on sections of a conduit segmented by computational nodes. Conservation of mass is represented by Equation 1, and is applied across a node. The staggered grid approach requires the conservation of momentum Equation 2 to be applied on a different control volume. The layout of these volumes is shown by the following graphic.

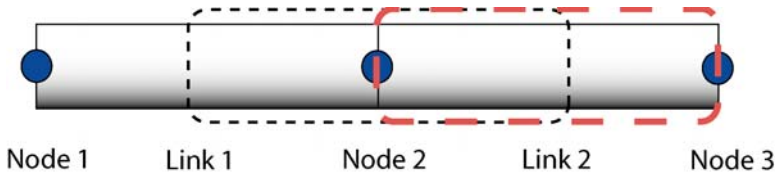

Figure 2 *SUPERLINK staggered grid computational scheme*

The control volume shown in short dashes illustrates the continuity equation for node 2, while the long dashed envelope indicates the momentum equation for link 2.

The St. Venant equations of motion only apply to free surface flow. This fact limits their application to pressurized flow, but switching to a closed conduit equation is often an unstable transition. As mentioned in the model review section, a common solution is to employ the “Priessmann slot” to extend the free surface equations to

conduits flowing full. Again, this slot area is not used for flow calculations, but merely to pressurize the conduit still being modeled by open channel flow equations.

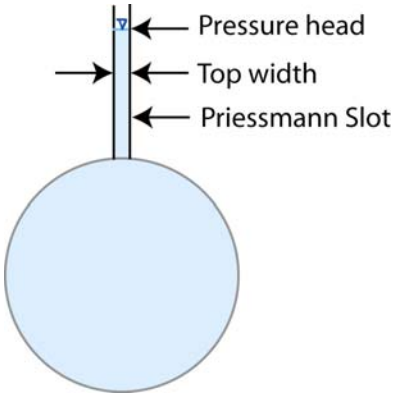

Figure 3 *Cross section view of pipe with Priessmann Slot*

Linearized Equations

To solve the partial differential equations, they must be discretized over their respective control volumes. Thus, unsteady terms such as flow rate and depth become time dependent variables. The discretized continuity equation with indices referring to Fig. 2 becomes

$$Q_2^{\,t+\Delta t} - Q_1^{\,t+\Delta t} + \left(\frac{B_2 \Delta x_2}{2} + \frac{B_1 \Delta x_1}{2} + A_{S1} \right) \frac{h_2^{\,t+\Delta t} - h_2^{\,t}}{\Delta t} = Q_{01} \qquad (3)$$

The momentum equation takes a similar form

$$\left(Q_2^{\,t+\Delta t} - Q_2^{\,t}\right)\left(\frac{\Delta x_2}{\Delta t}\right) + x_3 Q_3^{\,t+\Delta t} - x_2 Q_2^{\,t+\Delta t} + gA_2\left(S_{f2} + S_{L2}\right)\Delta x = gA_2 S_{02}\Delta x + gA_2\left(h_2^{\,t+\Delta t} - h_3^{\,t+\Delta t}\right)$$

(4)

The only new term in these equations is *B*, or the top width of flow area.

Boundary Conditions

As with any modeling problem, a set of boundary conditions must be applied to the extents of the network. With regards to the SUPERLINK model, these boundaries are located at the ends of each superlink, or junctions. The first component of the junction boundary is the water surface elevation (head). Junction heads may be known or unknown, as determined by the actual network configuration. A known junction head may be controlled by something external to the model, such as a reservoir at the network outlet. This feature would create backwater pressure propagating upstream, thus affecting flow upstream. Unknown junction heads occur at internal connections of two or more superlinks. Junctions representing an intake structure at the start of a superlink could also have an unknown head.

Flow into and out of these junctions, whether of known or unknown head, is governed by end condition boundary equations. Inlet entrance geometry governs pipeflow in steep channels, and exit properties can control in low gradient conditions. The end equations use the head in the junction as well as geometric variables to produce a set of coefficients for each inlet and outlet. The inlet and outlet coefficients by Ji (1998) were found to be unstable in certain situations and were reformulated as discussed in the model development section.

Solution Technique

The implicit scheme is defined by a simultaneous solution to all unknowns in the system at each time step. Instead of computing the head at every internal point (junctions and nodes) as the model steps through time, only unknown junctions are part of the

solution matrix. The reduction in the matrix size and thus computational demand is substantial. But the elegance of this routine is the way in which the unknown internal node depth and flow are incorporated into the junction matrix solution. Through a series of recurrence relations, the momentum and continuity equations are propagated throughout each superlink from one node to the next. This is done in both the forward and reverse directions in order to capture both positive and negative flow. The resulting coefficients become part of a relatively complex equation relating junction heads, superlink end conditions, internal node depth, internal pipe flow rate, and current timestep network inputs.

The matrix used to solve these equations takes the form as shown, and typically could exceed 200 x 200 in size.

$$\begin{bmatrix} F_{1,1} & \Phi & 0 & 0 \\ 0 & F_{2,2} & \Phi & 0 \\ 0 & \psi & F_{3,3} & \psi \\ 0 & \psi & 0 & F_{4,4} \end{bmatrix} \begin{bmatrix} H_1 \\ H_2 \\ H_3 \\ H_4 \end{bmatrix} = \begin{bmatrix} G_1 \\ G_2 \\ G_3 \\ G_4 \end{bmatrix} \qquad (5)$$

In this matrix, three main components are represented. First, the square matrix set is clearly of a sparse nature, but randomly so. The diagonal elements denoted by F and off-diagonal elements Φ and ψ all are summations of superlink coefficients (equations 30-33, Ji, 1998). The particular coefficients summed as well as their location in the matrix are dependent on the connectivity of the network. For example, a junction with only one superlink to or from would only see one off diagonal element, whereas a complex junction with multiple connections would have numerous off-diagonals. The second variable, H, is a one-dimensional array of heads at the future time step for each junction in the network. Third is the "right hand side" vector of the matrix equation. G is

composed of values from the current time step including junction head and boundary conditions, as well as junction inflows for the future time step.

With the matrix constructed, any number of solution techniques can be applied. The order of the left hand square matrix is equivalent to the number of junctions in the system. If the order becomes large (over 500) it would be prudent to consider efficient solving routines designed to utilize the sparse nature of the matrix. The location of non-zero elements is critical to reducing computation time. Although the majority of non-zero elements in this case will be diagonally biased, there are cases where an outlier would render some solution techniques useless. Thus the generalized LU decomposition solution method was chosen, which provides a full solution of a sparse matrix.

Model Development

SUPERLINK Algorithm

The actual coding of the SUPERLINK scheme initially appeared to be a trivial task. Ji's (1998) publication was carefully laid out to provide a step-by-step review of the model's formulation. The task of coding was undertaken in the computer language *C*. It soon became apparent that there were unforeseen difficulties in reproducing a functional code. The very nature of this implicit staggered method can be likened to an automatic transmission, contrasted to the "manual shift" finite volume concept. Although this may seem humorous, nothing was obvious about the numerics of SUPERLINK. It was extremely difficult to trace bugs in the developing code because numerical instabilities seemed to propagate from nowhere. Ji's (1998) algorithm was reproduced by following these general steps:

1) Calculate momentum and continuity coefficients for a superlink
2) Calculate forward recurrence relations for each node and link within the superlink
3) Calculate reverse recurrence relations for each node and link within the superlink
4) Calculate boundary condition coefficients
5) Using all of the above coefficients and recurrence relations, calculate a set of coefficients for use in the solution matrix
6) Repeat steps 1-5 for each superlink in the system
7) Calculate matrix values based on connectivity of the superlinks
8) Solve the sparse matrix
9) Based on the matrix solution of head at each unknown junction, calculate the flow at the upper and lower ends of each superlink

10) Solve for flow and depth in each pipe and node, repectively

11) Continue from step 1 with new flows and depths

Code testing and refining

Testing of the scheme began with the simplest network possible: one superlink connecting two junctions with known heads. The true test of index accuracy was to ensure that an equivalent flow was calculated in both forward and reverse directions after simply switching the boundary heads. Although depth is determined at nodes, area of flow is required at the center of the links to calculate flow. A depth at the midpoint of each link exists solely for the purpose of flow calculations, and is an average of adjacent node depths (Figure 4). Stability problems, particularly those related to flow reversal, were solved by revisiting the entrance/exit hydraulics as described in the following sections.

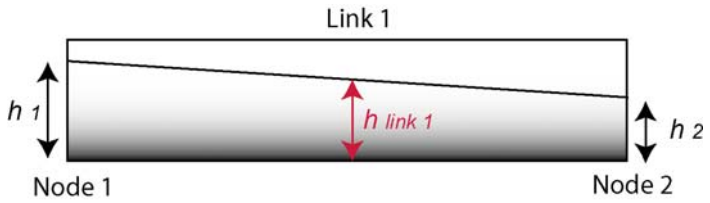

Figure 4 *SUPERLINK depth computation scheme*

Entrance hydraulics

The general equation for inlet-controlled flow is given as

$$Q = CA\sqrt{2g\Delta H} \quad (6)$$

where C is a geometric coefficient, A is the flow area, and ΔH is the difference in head between the supply reservoir (junction) and pipe (node 1, link 1). Ji (1998) had taken

entrance boundary equations from other sources, and thus the derivation could not be easily followed. Re-deriving the superlink end equations from Eq. 5 created an alternate set of boundary conditions. We define $\Delta H = H - h - Z_{inv}$ where H is the junction head, h is the depth at the first node, and Z_{inv} is the invert elevation of the first node. By squaring both sides of the flow equation we get:

$$Q^2 = C^2 A^2 g\left(H - h - Z_{inv}\right) \qquad (7)$$

The time varying Q is broken into the current time step and the future time step, and we solve for depth h. (Eq. 8) This process can be applied to the downstream end of a pipe as well to account for instances of backward flow. (Eq. 9)

$$h_u = \frac{|Q_u| Q_u^{t+\Delta t}}{C_u{}^2 A_u{}^2 g} + H_u - Z_{inv,u} \qquad (8)$$

$$h_d = -\frac{|Q_d| Q_d^{t+\Delta t}}{C_d{}^2 A_d{}^2 g} + H_d - Z_{inv,d} \qquad (9)$$

With these changes implemented in the code, the model ran with a very simple one-pipe network with known heads at either end junction.

Exit hydraulics

Like the pipe entrances, pipe exits were modified from Ji's (1998) algorithm to more accurately model various flow regimes. In exit hydraulics, four possible conditions must be considered for pipes flowing less than full. First, in a mild sloped channel where normal depth is greater than critical depth and junction head less than critical depth, the outfall depth is controlled by critical depth. Second, steep sloped channel exits where critical depth is greater than normal depth are governed at the exit by normal depth.

Third is a critical sloped channel where normal depth equals critical depth, critical depth is used for end control. Fourth is the case of backwater effects, when the depth in the downstream junction begins to affect depths upstream. To experience backwater effects, the head in the junction must exceed the head of critical depth (critical depth + invert elevation).

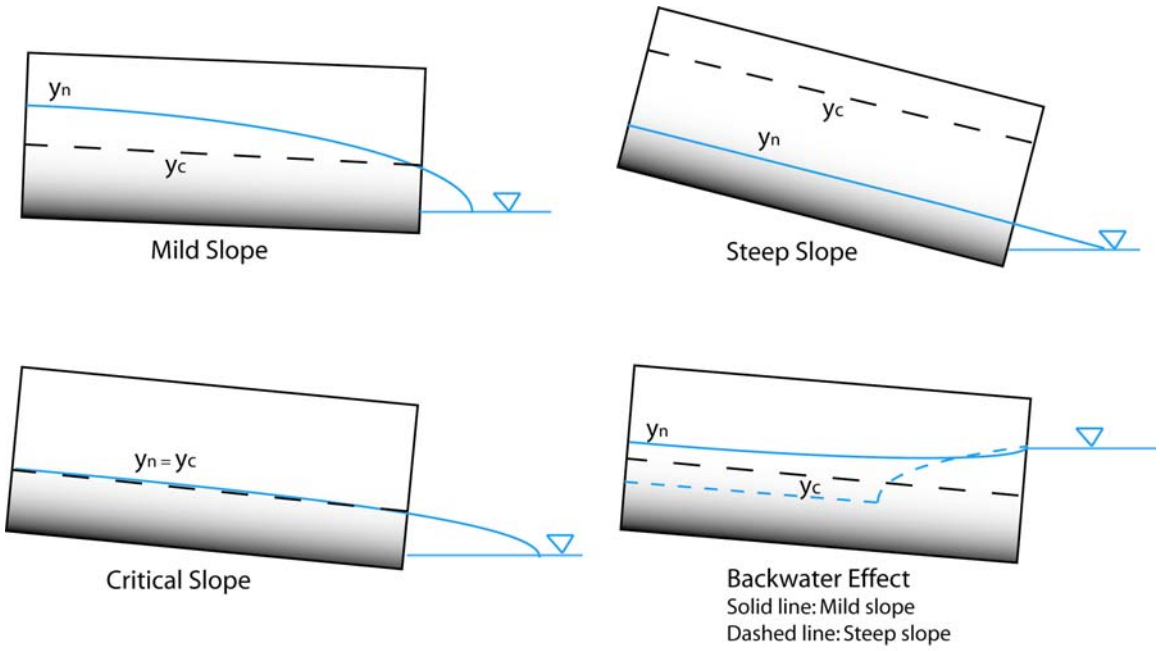

Figure 5 *Pipe exit conditions*

If the system is obeying conservation of momentum and the length of pipe is sufficient such that the friction slope is equal to the bed slope, the solved depth should be normal depth. Critical depth, however, must be calculated for the given flow rate and geometric variables. As the solution for critical depth is non-linear, the Newton-Raphson iterative solution technique was employed. This method searches for roots of an equation with a truncated Taylor series expansion to approximate F(x) for some guess x. In this case, the function F(x) is Manning's equation for open channel flow. (Eq. 10) Because the series

is truncated, the solution is not perfect. A correction is applied by Equation 11, where Δx is a correction to flowrate Q.

$$Q = \frac{1}{n} A R^{2/3} S_0^{1/2} \quad (10)$$

$$\Delta x = -\frac{F(x)}{\partial F / \partial x} \quad (11)$$

Iterations are performed until the correction Δx drops below a given threshold. (Mays, 1999). This process was imbedded into the code, and at each time-step the exit depth is checked against both critical depth and downstream junction depth.

Model Verification

To verify that the complete model was operating properly, Ji's (1998) test simulation for a simple six pipe network was reproduced. A boundary head at junctions D and F represented a tidal surge inducing backwater effects. Input at junctions A and C began after the tidal surge, allowing negative flow to occur. Positive pipe slope is denoted by the small arrows along each superlink.

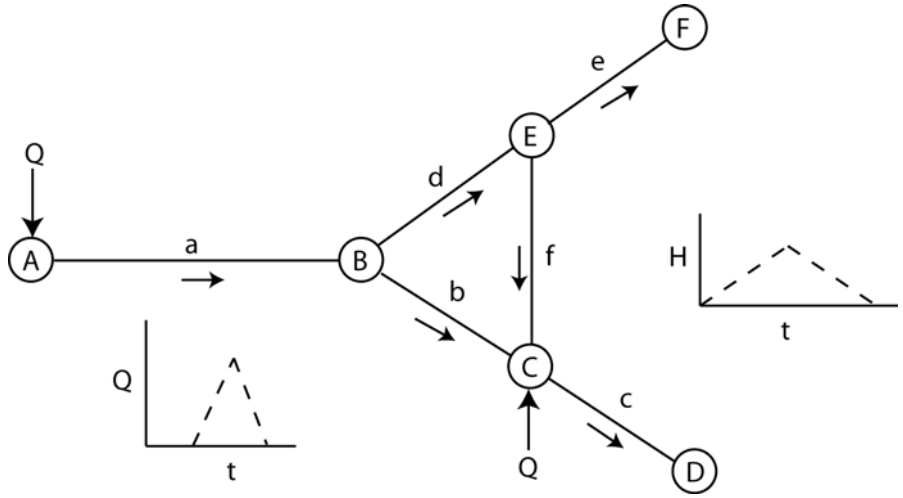

Figure 6 *SUPERLINK test case*

The following hydrographs matched those provided by Ji (1998). Reverse flow was present in all links at the start of the simulation due to the downstream boundary condition. To demonstrate the importance of looped network capability, pipe *f* flowed opposite its slope direction throughout the simulation because of a greater head at junction C than E.

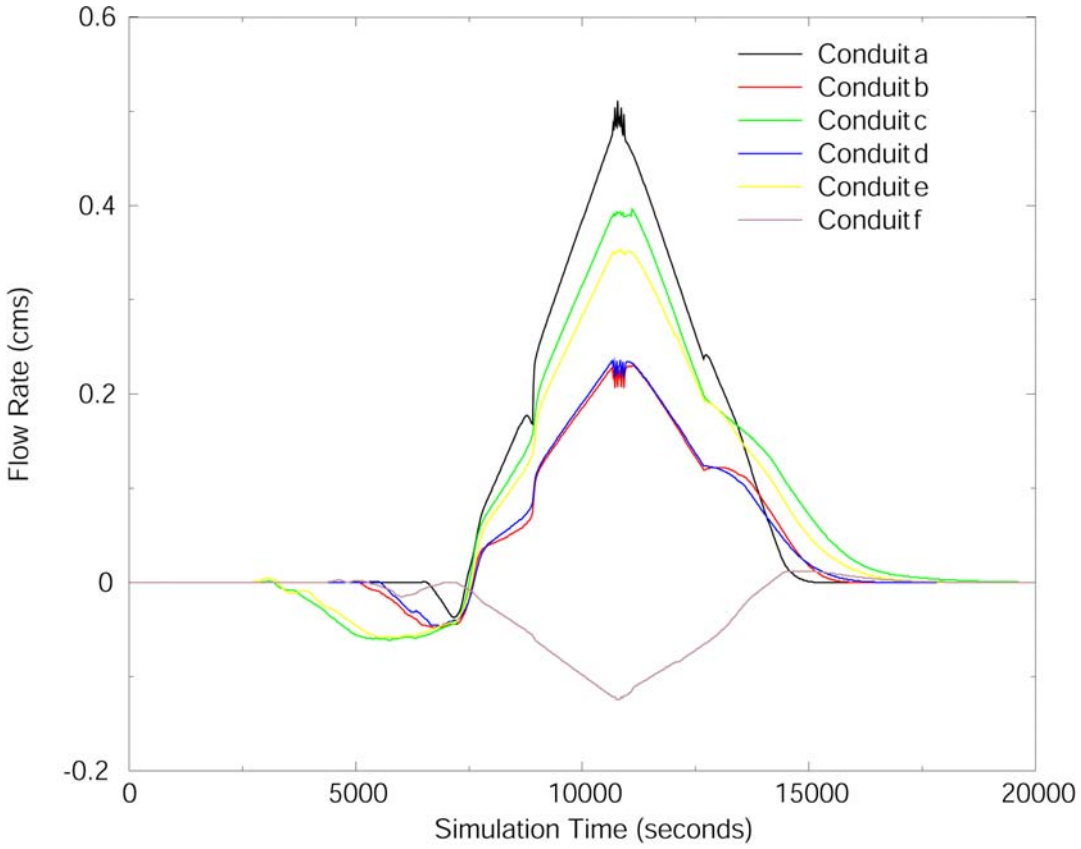

Figure 7 *Superlink demonstration simulation*

Changes to Model

As complexity was added to the test networks, additional deficiencies in the original formulation were discovered. One such instance involved the introduction of unknown heads to the model, thus incurring the use of the matrix solution. A mass

balance check indicated model connectivity problems, but once again it was extremely difficult to track the source of error. By process of elimination, it was discovered that the signs of two summations in a coefficient equation had been inadvertently switched in Ji's (1998) publication. In similar fashion another typographic error was found in an equation relating boundary conditions where a parenthesis had been omitted.

The last major hurdle dealt with initial conditions. The nature of equations 8 & 9 does not allow flow to move into the system when the area of flow is zero. It is therefore necessary to maintain a very small depth at the nodes even when flow is zero. A danger in imposing a depth is to create instability within the flow calculation, as physically these numbers should be simultaneously generated. Extensive testing found that an initial depth of 0.00001 m provided a stable minimum, allowing flow to commence without disrupting the mass and energy balance. This value is likewise imposed when inputs cease and a network drains, simply to keep the pipes "wet".

GSSHA and SUPERLINK

Linking Models

With a robust set of options comes complexity, hence the GSSHA code greatly encourages new subroutines to run side by side instead of attempting to imbed the processes. This was beneficial at the development stage (as testing could be limited to SUPERLINK exclusively) as well as the linking stage (see Appendix A).

Linking the two models presented a challenge in simulating hydrologic processes on a wide range of scales. Typical GSSHA grid sizes are on the order of 10-30 meters, which is usually suitable for modeling catchment scale processes such as infiltration, evaporation, overland flow, and channel flow. However, it became apparent that grate inlets function by micro-topography, as curbs and crowned road profiles direct flow to the catch basins. This scale of hydrology cannot be represented on even a 10-meter grid, so it was necessary to develop a conceptual relationship between GSSHA and SUPERLINK to realistically introduce flow to the storm drainage network.

Grate Hydraulics

Some simplifying assumptions were necessary to simulate the intake process feasibly. It is reasonable to assume that most inlet points are located at depressions or curbs of a crowned roadway. Although this certainly is not true in all cases, the vast majority of the catch basins fit this description. GSSHA considers planar sloping grid cells with a depth of ponded water for the case of overland flow. At each intake point, SUPERLINK is given the number of grates represented by a node (N = 1 to 4). The

potential flow intake available to SUPERLINK (q_{in}) is then taken as a percentage of total ponded volume (V_{cell}) based on the number of grates per time step (dt) by the equation

$$q_{in} = \frac{N\alpha V_{cell}}{dt} \quad (12)$$

where $\alpha = 1/N_{max}$. This simplification follows the reasoning that a cell with four grates would be capable of intercepting all of the ponded water.

Surcharged manholes & grates

It is clear that the storm drainage network and the land surface scheme must interact in such a manner as to allow surcharged manholes and grates to discharge back to the surface. As the SUPERLINK model will run in parallel with GSSHA, this interplay is easily accounted for. Each time SUPERLINK is called, the depth in the cells containing manholes and grates will be passed to the subroutine. SUPERLINK determines whether there is sufficient space in the structure to accept all flow available from the grate hydraulics calculation. If so, this volume will be subtracted from the overland flow plain and added to the subsurface network. Otherwise, the flow will be forced to continue on in the overland plane, thus simulating a system operating at full capacity. If SUPERLINK calculates the head at a manhole to be greater than the ground surface elevation or overland flow head, the excess volume will be subtracted from the drainage network and added to the surface cell. By following this method at each timestep, SUPERLINK and GSSHA will interact realistically.

IV. METHODOLOGY

Data for the Modeling Study

It was necessary to model a watershed with a significant urban presence and subterranean drainage network to fully test the routines. A low gradient topography would provide situations of inundation and pressurized pipes. But perhaps most critical was the availability of a quality dataset including: rainfall records, stream flow records, digital elevation model (DEM), land-use coverage, stream channel and storm drainage network data. All but one of these requirements could be readily met by Dead Run, a 14.3 sq km watershed in Baltimore, Maryland.

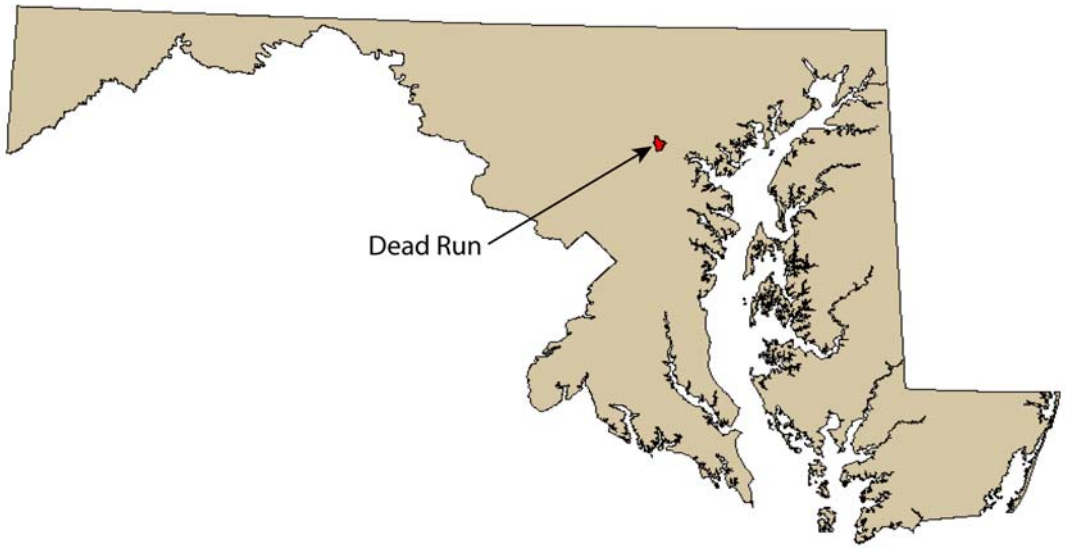

Figure 8 *Maryland with location of 14.3 km^2 Dead Run watershed*

Bounding UTM Coordinates: 4355809 – 4349732 N, 347633 – 352363 E

Extensive field work has been ongoing as part of a study by researchers from Princeton University. Precipitation data were derived from the WSR-88D radar in Sterling, Virginia (75 km from watershed center) and a network of 19 rain gages.

Discharge data at the outlet of Dead Run is provided by a USGS gaging station. The Princeton group has obtained GIS layers of land use, a 10 meter DEM, and drainage maps from the county of Baltimore. Their own field campaigns have involved cross section measurements of stream channels, rating curve measurements, and soil infiltration testing. The basin also includes a number of small to medium sized detention basins. Only one element required a significant amount of work: the drainage network.

Storm drainage network

The three maps that covered this watershed contained a plan view of the network with symbols for catch basins, manholes, outlets, and pipe sizing. To produce pipe data for use in the SUPERLINK scheme, it was necessary to scan and georeference these images. Following is an example of the scanned image and resulting digitized network superimposed on the GIS land use map. The GIS landuse map (Figure 10) also shows the remarkable level of detail available for this watershed.

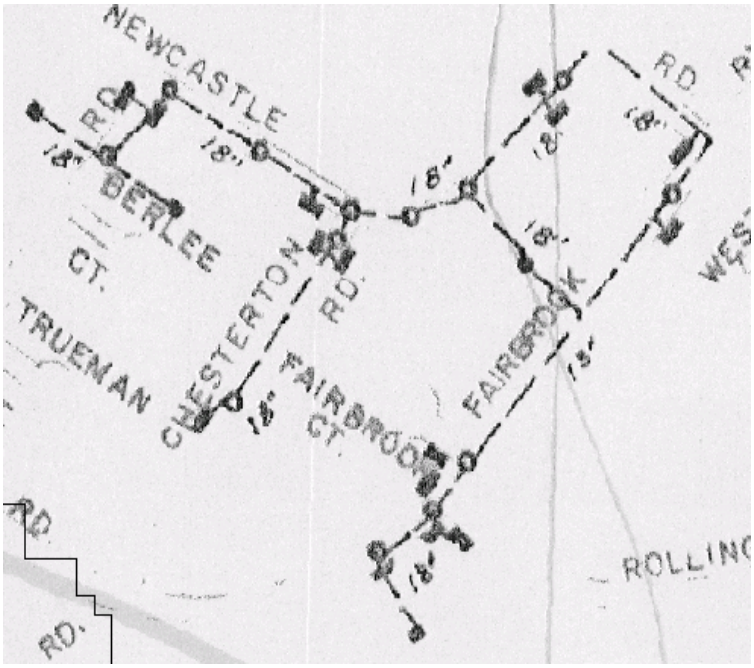

Figure 9 *Scanned drainage map*

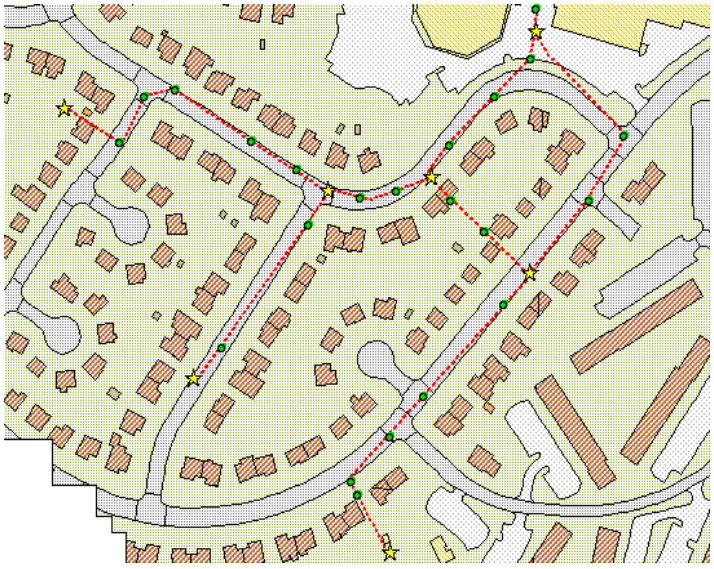

Figure 10 *Digitized drainage map*

The storm drain maps were created independently of the current GIS road and building layers, and did not overlay each other perfectly. This is due to the fact that the pipe network scans were from paper maps created by hand and not tied to a coordinate

system. For overland flow in GSSHA and pipe flow in SUPERLINK to interact realistically, network intake points (catch basins) should coincide with impervious roadway coverage where applicable. Thus the location of specific network elements had to be shifted slightly to accurately represent the existing conditions. Junctions are shown with star symbols, nodes (catch basins and computational points) by open circles, and superlinks by dashed lines.

The numbering scheme required by SUPERLINK is discussed in the appendix. Junctions, links, and nodes were created as GIS layers in ArcView to represent pipe intersections, pipes, catch basins, and outlets. Because this was the first use of the storm drainage model, all dataset preparation was done manually to determine the exact creation process of the input file. For this scenario, all calculations were performed using points (junctions and nodes) with associated tables listing downstream pipe size. Connectivity information was contained within line layers that simply denoted the upstream and downstream junction number. Final assimilation of this GIS data is further described in Appendix B.

Pipe invert elevations were not readily accessible for the Dead Run catchment except in detailed engineering drawings. Due to the amount of data being processed, a simplifying assumption was used to calculate the invert of each pipe. It is reasonable to assume that a typical subterranean network largely follows the ground surface based on pipe installation limitations. With this in mind, ArcView was used to assign a ground surface elevation to each point from the DEM. Using a typical pipe depth of 2 meters, an invert was calculated from the surface elevation. Where it was obvious that this

simplification defied engineering practices, the invert elevations were modified to produce positive slopes in the assumed flow direction.

Hurricane Isabel

The drainage network will have its most pronounced effect during a moderate to high intensity storm, and therefore the event of September 18-19, 2003 was selected as the model test case. Hurricane Isabel was classified as a Category 2 when it struck the North Carolina coast, but weakened to a tropical depression as it moved north. The storm dropped heavy rainfall on much of the east coast, including Maryland and the Baltimore watershed of Dead Run. As is common in hurricane precipitation patterns, Baltimore received two strong pulses of rainfall 150 minutes apart (Figure 11). The peak discharge recorded by the USGS gaging station at the outlet of the watershed was just under 40 cms (~1400 cfs or 10 mm/hr), and significant flooding was reported on the North Branch of the Potomac River. Basin averaged rainfall peaked at 53 mm/hr, but localized cells of intense precipitation were recorded above 200 mm/hr. Thus the distributed nature of the rainfall input is as critical as the distributed landuse and soil classification. This event was selected because it allows calibration of GSSHA using the observed precipitation and stream records.

A brief analysis of the volume of rainfall versus volume of discharge in each peak highlights a problem. There is 25% less precipitation in the second pulse versus the first, but only 9.5% less runoff volume for the second peak of the hydrograph. If the initial conditions were unknown, this imbalance could be attributed to dry soil conditions leading up the first peak. However, the steady period of light rain in the hours preceding

the storm reduces this possibility. The model results will demonstrate this apparent deficit in greater detail and point to radar bias as the problem.

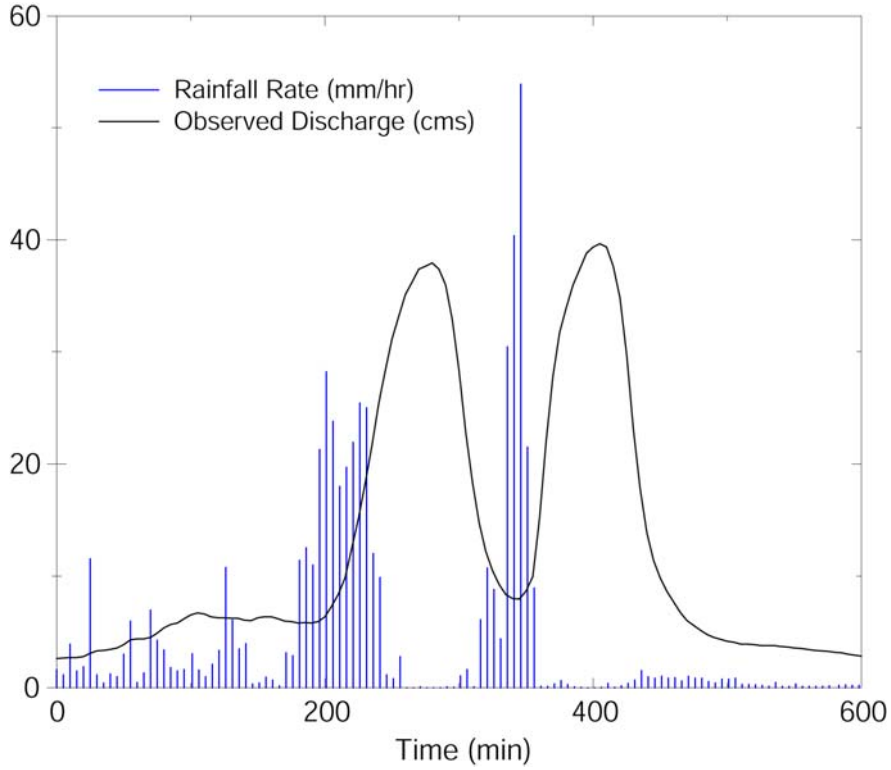

Figure 11 *Basin average rainfall with observed discharge record*

Figure 12 provides a sense of rainfall intensity compared to the infiltration capacity of the soil. Rainfall records prior to the simulation period are similar to the period from 0 to 150 minutes, or nearly equal to the saturated hydraulic conductivity. This observation is useful in initializing soil moisture. The longer first pulse of rainfall produced moderate runoff, while the shorter second pulse generated somewhat more intense infiltration excess. Although the storm had periods of remarkable intensity, storm total accumulation was only 66 mm (2.6 in) and therefore is not categorized as an extreme event.

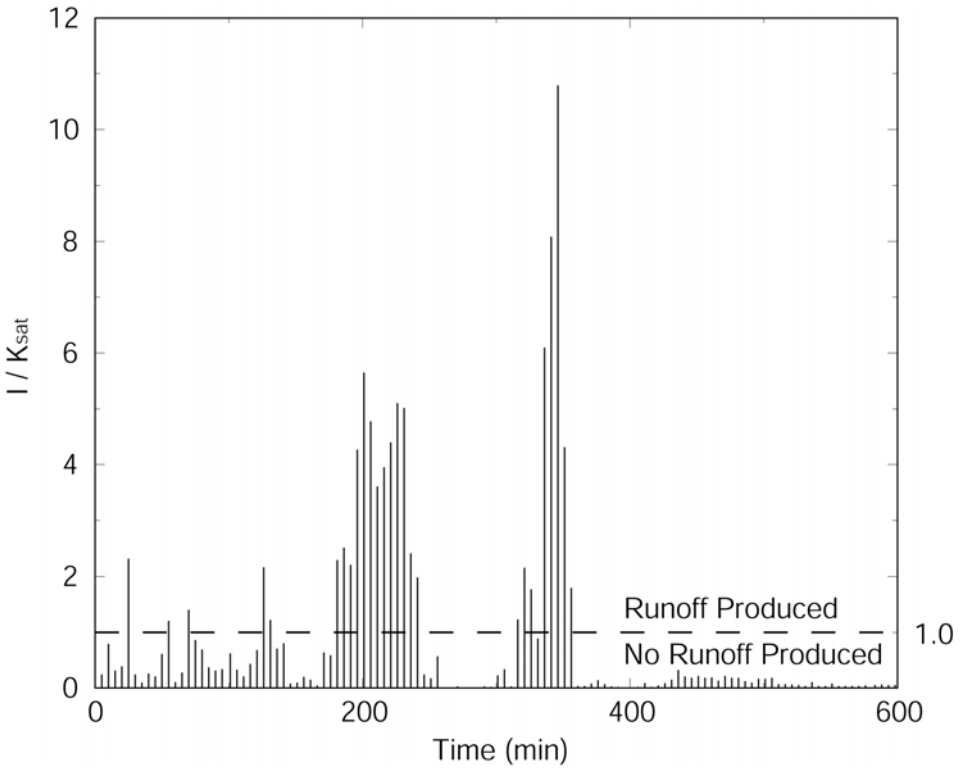

Figure 12 *Basin average rainfall normalized by saturated hydraulic conductivity*

As previously mentioned, radar data from Sterling, Virginia was provided at 1 km spatial and 6 minute temporal resolution, and overlays the Dead Run watershed as shown.

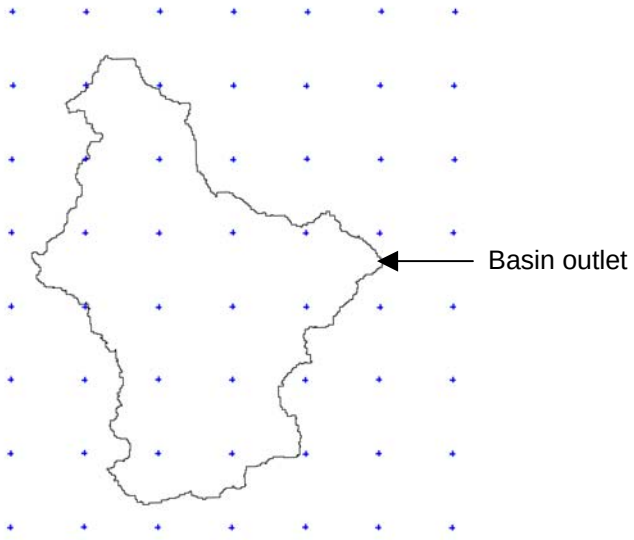

Figure 13 *1 km radar grid overlaying watershed (south-east corner of each cell shown)*

Parameter Assignment

Gridded Watershed

With the modeling data in various formats, the last step is to assemble the components for use within the modeling framework by means of the aforementioned Watershed Modeling System, or WMS. This software is capable of transforming polygon, line, and point data into gridded maps, which are then read by the GSSHA routine. Initial efforts were focused on a 10 meter grid size, as this matches the resolution of the DEM from Princeton. However, each hydrologic process must be executed on the resulting 143,000 grid cells (within the 14.3 sq. km watershed), and this is computationally expensive. Also, gridded models are subject to artifacts in the DEM that do not allow the land surface to drain properly. Removal of this "DEM noise" is much more difficult at 10 meters compared to 30 meters, because the larger grid size is smoothed during aggregation. A 30 m grid size reduces the number of grid cells to approximately 16,000, is free of artifacts, and thus was chosen for the initial watershed simulations.

A landuse classification index is then assigned to each grid cell based on the majority coverage overlaying it. Tied to each index value are hydrologic parameters such as saturated hydraulic conductivity, roughness, porosity, initial moisture content, and capillary head.

Table 1 *Summary of Dead Run landuse*

Land Use Classification	Area (km^2)	Percent of Watershed
Road and Parking Lot	1.57	11.0%
Building Rooftop	3.54	24.8%
Grass/Woodland	9.19	64.2%

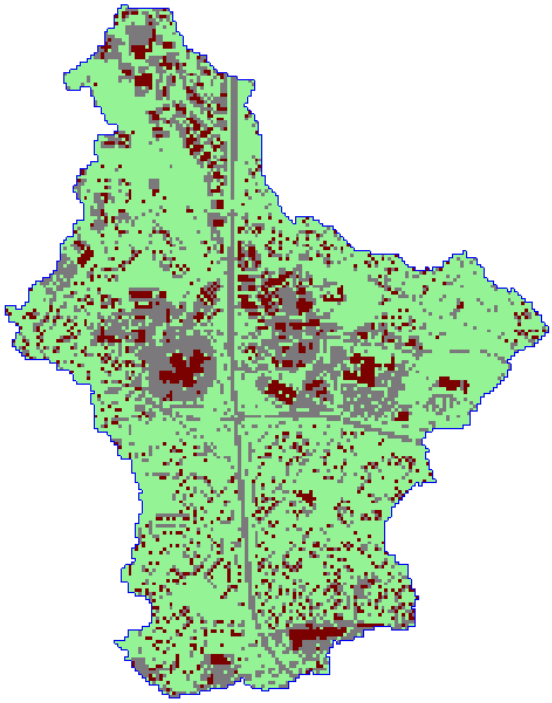

Figure 14 *30 meter gridded landuse map*

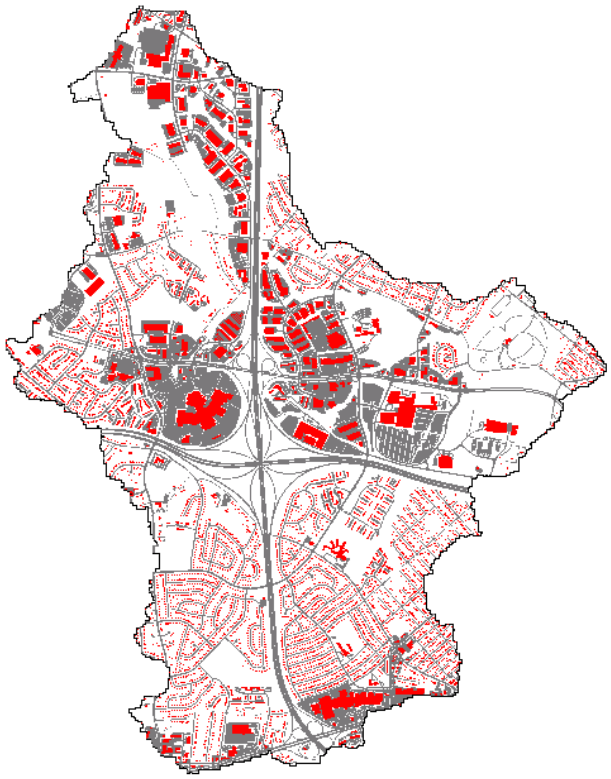

Figure 15 *GIS landuse map*

The gridded landuse index map (Figure 14) retains the major features of the watershed seen in the GIS map (Figure 15). Even at the 30-meter scale, the highway that divides the watershed into quadrants is still clearly visible as well as the large buildings and parking lots. Somewhat less distinctive are secondary roads and residential dwellings. Despite the loss of resolution due to coarsening, analysis of the relative influence of model components will still be accurate.

Width Function

The effects of drainage density have long been hypothesized, but the powerful distributed nature of this model provides an opportunity to simulate various degrees of modifications and compare their relative hydrologic response. To quantitatively report the degree to which a watershed is drained is not trivial task, because the measure must take into account not only the absolute number of flow links but also their length to the outlet. For example, a watershed may have a dense network of channels, but if arranged in a sinuous fashion will respond very differently to a basin with the same drainage density but straight channels. Thus the width function is employed to develop a measure of both drainage characteristics. For this research, the width function is defined as the number of flow segments at a given distance from the watershed outlet. A flow segment is defined as a 10 m length of either channel of storm sewer. The distance is measured along the channels and sewers themselves, thus representing the length a drop of water must flow to the exit.

Three scenarios have been considered to explore the effect of the width function: natural conditions, the modified channel network, and the current channel network with

storm sewers. To simulate the pre-development channel configuration, the WMS routine TOPAZ (Garbrecht and Marz, 1993) was used to calculate flow accumulations. This algorithm simply determines the surface area that drains through any given cell. Given a threshold value, WMS then creates stream arcs from cells with a contributing drainage area above this minimum. This approximation of natural conditions is shown in the following Figure 16, overlaid on the complete existing network. The second and third cases are shown in Figure 17, with channels in blue and storm sewers in red.

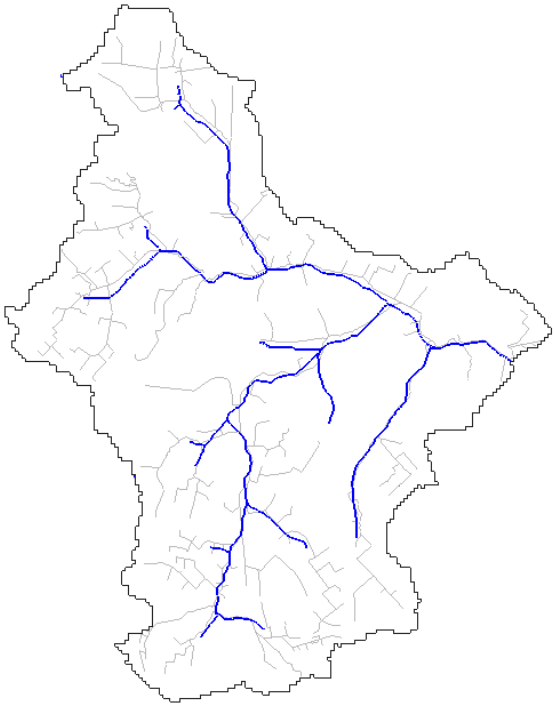

Figure 16 *Idealized natural network*

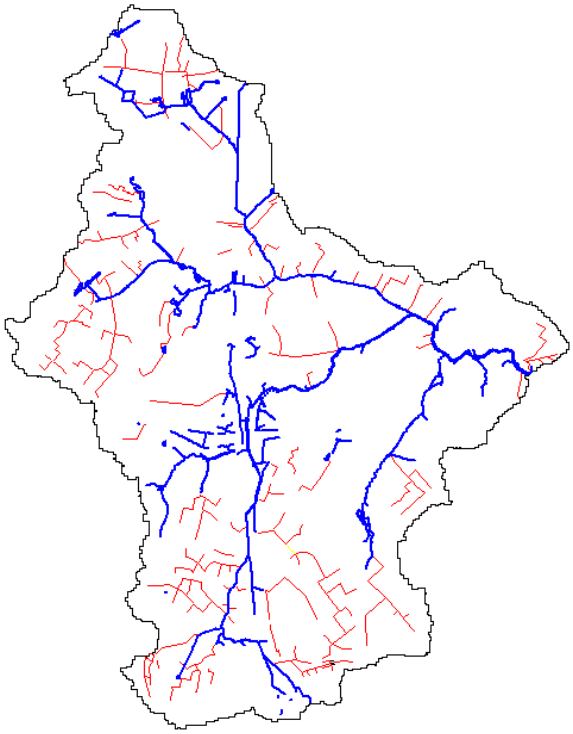

Figure 17 *Existing channel network in bold, storm drainage network in thin lines*

The width function, plotted against the distance from the outlet in Figure 18, provides a tool to qualitatively assess the modifications of the basin drainage. Comparing the natural and existing channel histograms, little deviation occurs until approximately 4000

meters. At this point, the modified channels display a significant increase in the drainage density. A visual inspection of the change in blue lines from Figure 16 to Figure 17 explains the difference: numerous channels were installed in the central core of the watershed. The existing channel plot also extends 1000 meters beyond natural conditions, due to an apparent extension of the channels farthest from the basin outlet. Figure 18 shows that expansion of the open channel network has a significant impact on the width function.

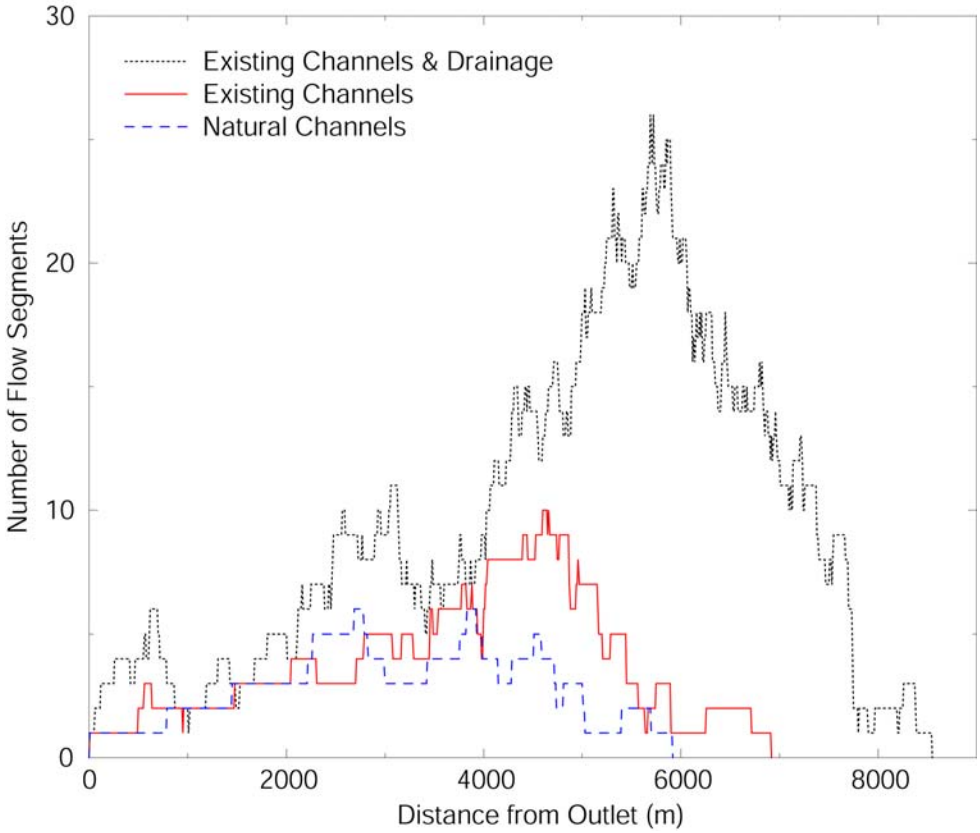

Figure 18 *Effect of drainage network on width function*

The effect of storm drainage on the width function is extremely pronounced. Once again, notable increases over the existing channels can be matched to heavily sewered areas in Figure 17. The strongest impact again falls beyond 4000 m, and not

coincidentally. In regions where the channels have been modified, it is likely evidence of intensive land development, which is often accompanied by the installation of subterranean drainage. By inspection of the drainage map, regions in the south and west of the watershed have the highest density of sewers. This is reflected in the width function, with a drastic increase in the number of flow segments past the corresponding length of 5000 m. However, conclusions on the effect of the increase in density must include mention of conveyance. The conveyance *K*, or quantity of flow a given segment can pass, is much less in the storm drainage pipes than in natural channels.

$$K = \frac{1}{n} A R^{2/3} \qquad (12)$$

In this equation, *n* is Manning's roughness coefficient, *A* is the bank-full flow area, and *R* is assumed to be the bank-full flow hydraulic radius. For pipes, conveyance is calculated at full flow conditions as well. The influence of conveyance can be significant. For example, a trapezoidal channel 1 m wide has a conveyance of 400, compared to a 0.45 m pipe's conveyance of 1.5.

By weighting the width function by conveyance, the segments no longer have equal count values. Though the large order streams near the outlet may be few in number, they will have a much larger conveyance sum than the numerous first order streams. Although the increase in density seen in Figure 17 represents lower capacity segments, they are still apparent in the conveyance weighted plot.

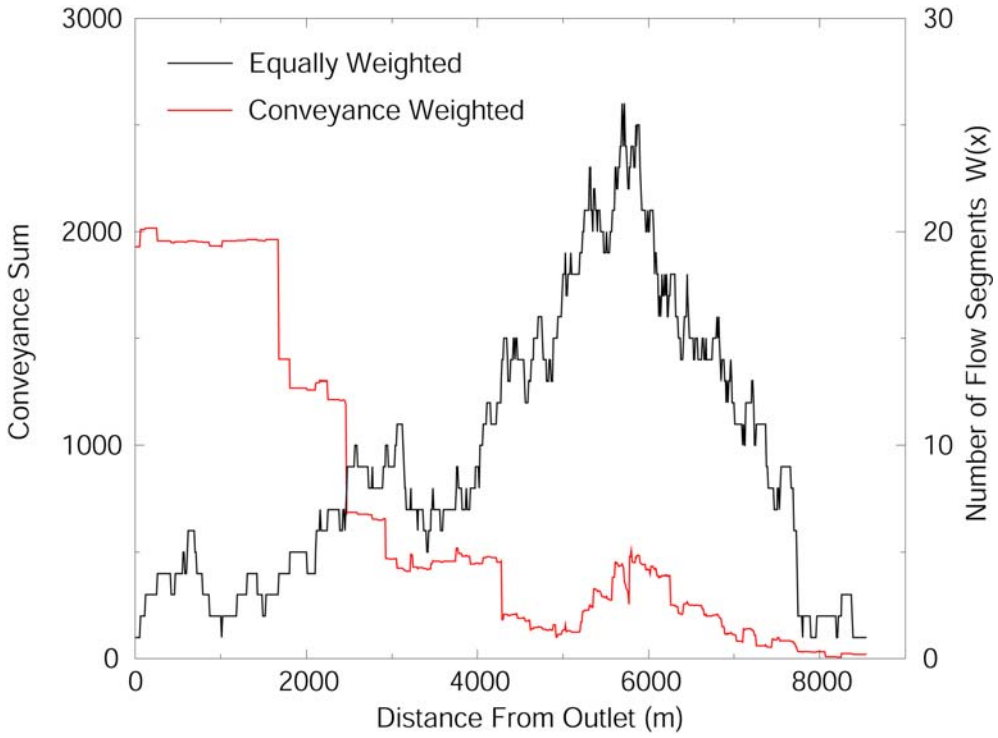

Figure 19 *Comparison between normal and conveyance weighted width functions*

The increase in drainage density may also be offset by another feature that appears in the width function plot. The majority of the density increase occurs beyond a distance where the natural system registered flow segments (6000 m). This can be explained by the indirect routing of small elements of the drainage system. Hence, a longer distance of travel to the outlet will partially suppress the response time effect of dense drainage.

Hydrologic processes

The importance of various hydrologic processes to a modeler depends on the focus of the modeling effort. Long-term simulations are heavily influenced by groundwater contributions to streamflow and climatic factors such as evapotranspiration losses. Single event simulations targeting flood peaks and timing rely mainly on the

short-term processes of infiltration, overland flow routing, and channel routing. Additionally, the effect of lakes and hydraulic structures are important for both long and short-term simulations. As the focus of this study is the effect of drainage network modifications, the model components will include the processes fundamental to single events.

Setting hydrologic parameters in GSSHA utilizes both values from the literature and past experience with the model. Saturated hydraulic conductivity, roughness coefficients of landuse, and initial soil moisture are the key parameters for the processes involved in a short-term simulation. One soil type was used throughout the watershed because soils data were not readily accessible. Of the two soil parameters, the model is most sensitive to saturated hydraulic conductivity, and thus it becomes the calibration parameter. As for the other soil parameter, because the simulations were begun after a period of steady light rain, the soil surface was assumed to be saturated.

Roughness coefficients influence the travel time across overland flow planes and in the channels. Their values were estimated from past experience with GSSHA modeling as well as published values. Overland flow Manning's roughness coefficients were set at 0.400 for the overland plain and 0.050 for roadways and parking lots. The disparity between these two values illustrates the vast difference between paved and natural surfaces. In contrast to the roadways and parking lots, a rooftop area roughness coefficient of 0.800 simulates the delay due to gutters and roof drains. Both of these surfaces do not experience infiltration, but the runoff response from roofs is substantially slower than pavement. Once runoff reaches the channels, a typical value of 0.04 is used for channel routing based on a clean, winding stream (Chow, 1988).

Model Calibration

To validate the joint model formulation, the GSSHA outflow hydrograph was compared to the USGS observed discharge record at the basin outlet. Saturated hydraulic conductivity was varied between 0.1 and 0.8 cm/hr as simulation results were compared to the observed plot. Figure 20 displays the final simulation with a K_{sat} value of 0.5 cm/hr. The model is most sensitive to $K_{sat,}$ and the final value was chosen for its ability to produce a first peak of 40 cms. Increasing K_{sat} to 0.8 cm/hr reduce this first peak by almost 25%.

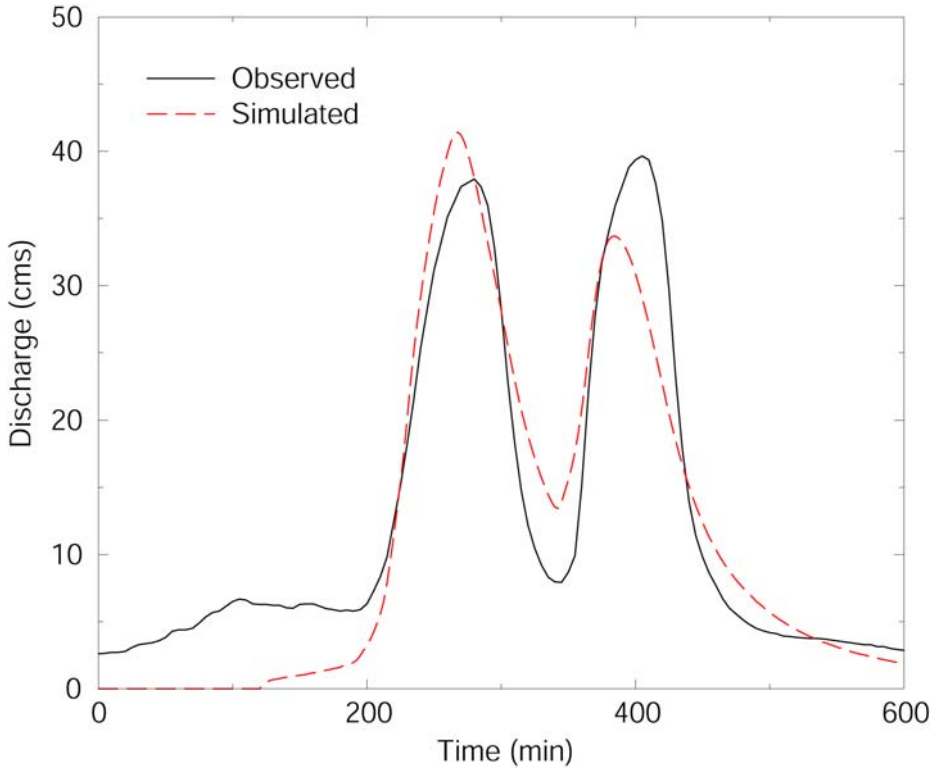

Figure 20 *Calibration of GSSHA on Dead Run*

It is evident that this "manual calibration" did not produce a perfect match to the observed hydrograph. A system such as Shuffled Complex Evolution would give a better parameter set by simulating thousands of combinations of variables within a set range.

But parameters are not the only reason for the inability of GSSHA to match the hydrograph, and more specifically the second peak. Recalling the discussing of precipitation volume versus runoff volume from the model data section, the volume of rainfall in the second pulse was significantly less that the first pulse while their runoff volumes were almost the same. The most likely explanation of this is radar underestimation. Radar data are almost always correlated to gage data by a bias adjustment. A mean field bias between radar and gage data was used by the Princeton group to adjust the radar-derived intensities by the following equation $r_a = 1.51 r_o$ where r_a is the adjusted rate and r_o is the observed rate. Also, radar reflectivity level is capped at specified decibel value (55 dBZ) to prevent highly reflective hail from giving unreasonably intense rainfall rates. In the case of Hurricane Isabel, it is highly probable that a combination of these two factors produced a radar dataset without enough rainfall during the second phase of the storm. Without question the highest intensities occurred during the latter pulse, thus subjecting these rates to the potential of being clipped and or dampened by the mean field bias. Ogden et al. (2000) showed that applying one radar bias value to a multi-pulse storm does not agree well with gage data for individual pulses.

The four detention ponds simulated were based on rough approximations of size, outlet structure, and discharge curves. A better understanding of the ponds and their attenuation characteristics might significantly improve modeling results. In similar fashion, a thorough geometry of the channels was not known, thus introducing another possibility for model misrepresentation. Shortcomings due to data in the model calibration are not as critical as if the watershed of interest were being simulated for

design purposes. Rather, its utility lies in the ability to simulate one catchment with varying drainage densities and properties.

V. RESULTS & DISCUSSION

Storm Drainage Network

With the model development complete, it is now possible to step through an idealized timeline of the urbanization of the Dead Run watershed. From the estimated natural conditions to current developed and drained conditions, it is possible to simulate the effect of separate and joint modifications to the basin. Outlet hydrographs will demonstrate the effects of man-made hydrologic features including channel modifications, detention basins and culverts, storm drains, and impervious area.

Channel Modifications and Detention Basins

Simulating the pre-development watershed is clearly a subjective task. It is impossible to reproduce every hydrologic feature that existed, say, 200 years ago. There are some approximations, however, that can be made based on typical development trends and existing topography. As mentioned earlier, the channel network for this simulation was derived from a flow accumulation algorithm. The width and depth of these "natural" channels were assigned identical values to the modified network to avoid storage-related differences. The one property given a slightly different value was the roughness coefficient. Urbanized channel networks often are intensively maintained, reducing flow attenuating material such as brush and long grass which might persist in a natural channel. They also tend to be straighter and more efficient than a naturally formed channel. Thus a Manning's n of 0.05 was used rather than 0.04, as recommended by Chow (1988).

Three networks were simulated without the existing impervious areas so as to remove land surface factors from influencing a strictly channel comparison. Figure 21 shows three conditions: “natural” channels, expanded channel network as exists currently, and current channel network with existing detention basins and culverts.

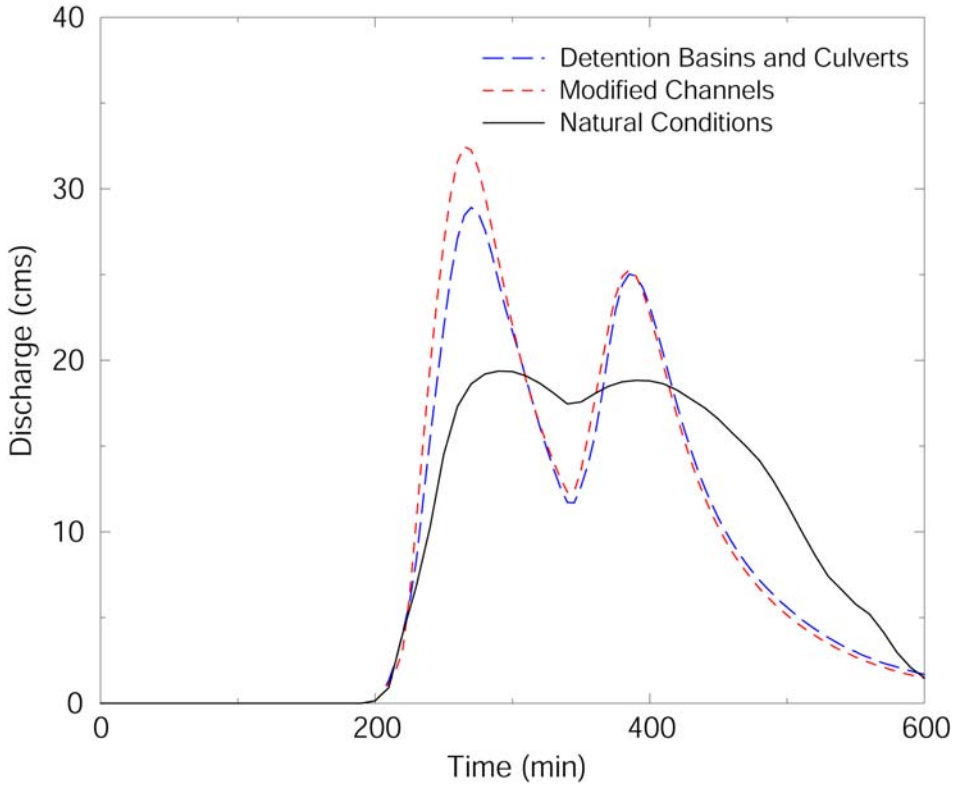

Figure 21 *Effect of modified channels on non-impervious watershed*

Most striking about Figure 21 is the change from a pre-development watershed to modified channels. The first flood peak increases by 67%, as runoff volume decrease minimally (2.5%). Comparing the thick line channels in Figures 16 and 17, as well as their corresponding width functions in Figure 18 provides clear evidence that increases in main channel density has a profound effect on the hydrograph. The addition of lakes and culverts reduces the peak discharge to a 50% increase over the natural case. This behaves

as expected due to the storage capacity of these small detention ponds and the attenuating effect of road culverts.

Table 2. Model results of channel modifications, no imperviousness

Scenario	*Peak Discharge (cms)*	*Time to First Peak (min)*	*Discharge Volume (m^3)*
Natural Channels	19.3	295	322,000
Modified Channels	32.3	266	314,000
Lakes & Culverts	28.9	270	303,000

Time to the first peak is decreased by the modifications to the channel network (Table 2). Because there is no impervious coverage in these scenarios, runoff from regions of the watershed without any channels is significantly delayed. Despite the fact that no imperviousness exists in these three scenarios, increased drainage density is able to convey runoff quicker than overland flow.

Storm Drainage Network

The next phase of simulations includes the existing network of modified channels, distributed impervious coverage, subsurface drainage, and detention ponds. Of particular interest is the performance of the storm sewer component, and ultimately its effect on the hydrology of Dead Run. A subset of the 268 links has been selected to display typical pipe flow hydrographs (Figure 22). The majority of pipes are first order, receiving all input from surface grate structures (solid lines). The increasing length of dashes on the pipe hydrograph lines represent increasing order pipes, accepting inflow from both upstream pipes as well as inlet grates. The pipe hydrographs have a remarkably quick

response to the rainfall, and are largely drained before the peak discharge reaches the outlet.

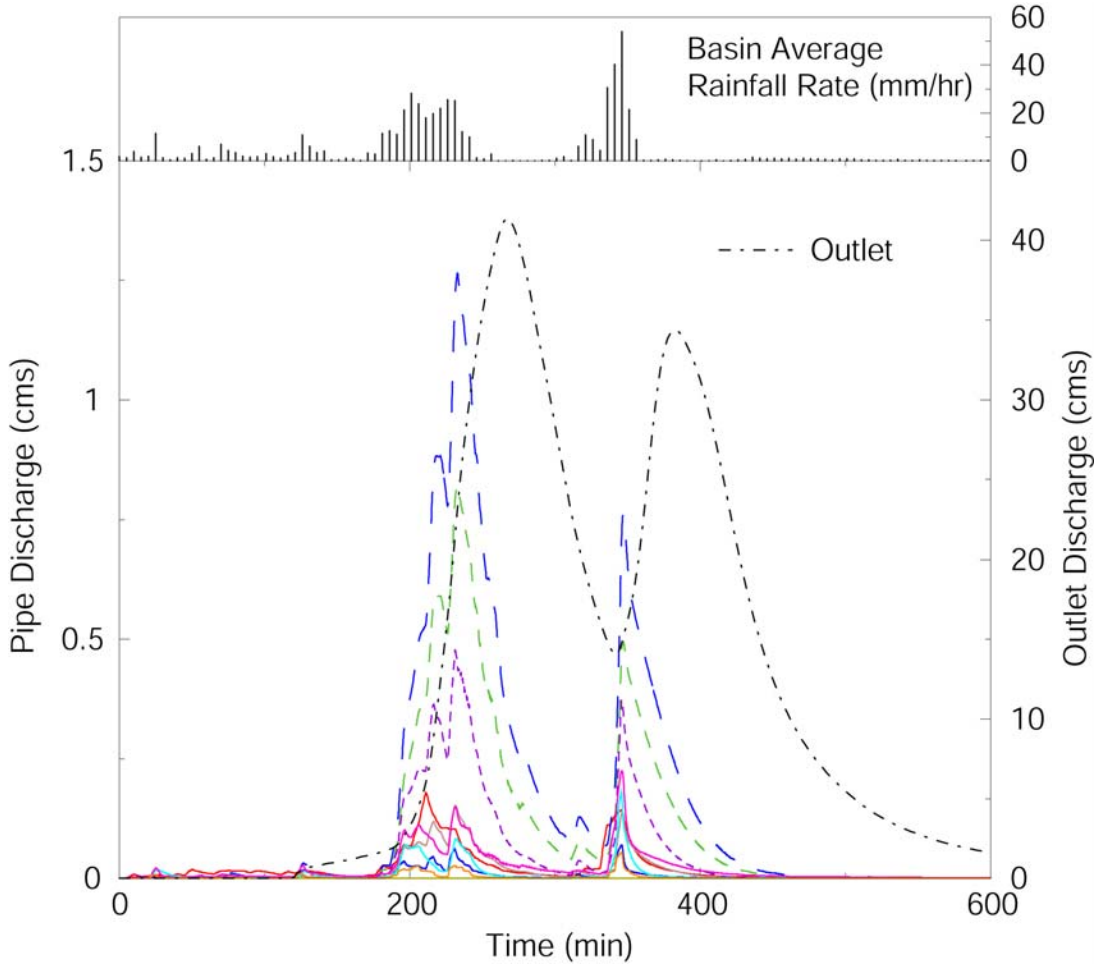

Figure 22 *Outlet and sample pipe discharge hydrographs, longer dashes represent higher order pipes*

The basin average rainfall hyetograph has been provided at the top of Figure 22 for comparison with pipe flow. The principal observation from this is the pipe flow during the period of intense rainfall during the second pulse at ~350 min. This can be explained by subsurface hydraulics. Once pipes become full and flow under pressure, they are unable to accept additional input. Also, pressurized manholes and intake grates behave as outlet points when the head exceeds the ground surface elevation. Thus this

period of extraordinarily heavy precipitation (local cells up to 200 mm/hr) overwhelms the network and much of the runoff remains on the surface. Although the first storm pulse also produced high rain rates, the storm sewers were able to accept most of the water available at the intake grates.

To fully explore the hypothesis that storm sewers become overwhelmed and have less of an effect on extreme events, the 1997 event that caused flash flooding in Fort Collins, Colorado (Ogden et al., 2000) was simulated over the Dead Run watershed. This four-pulse storm dropped 14.98 cm (5.9 in) of rain in 4 ½ hours, more than doubling the flood peak of the Dead Run outlet hydrograph compared to Hurricane Isabel. Although the draining of the basin was slightly enhanced as seen in Figure 23, the flood magnitude was unaffected. The limited conveyance and intake potential of the drainage network could not enhance flow routing to the outlet enough to raise the peak discharge.

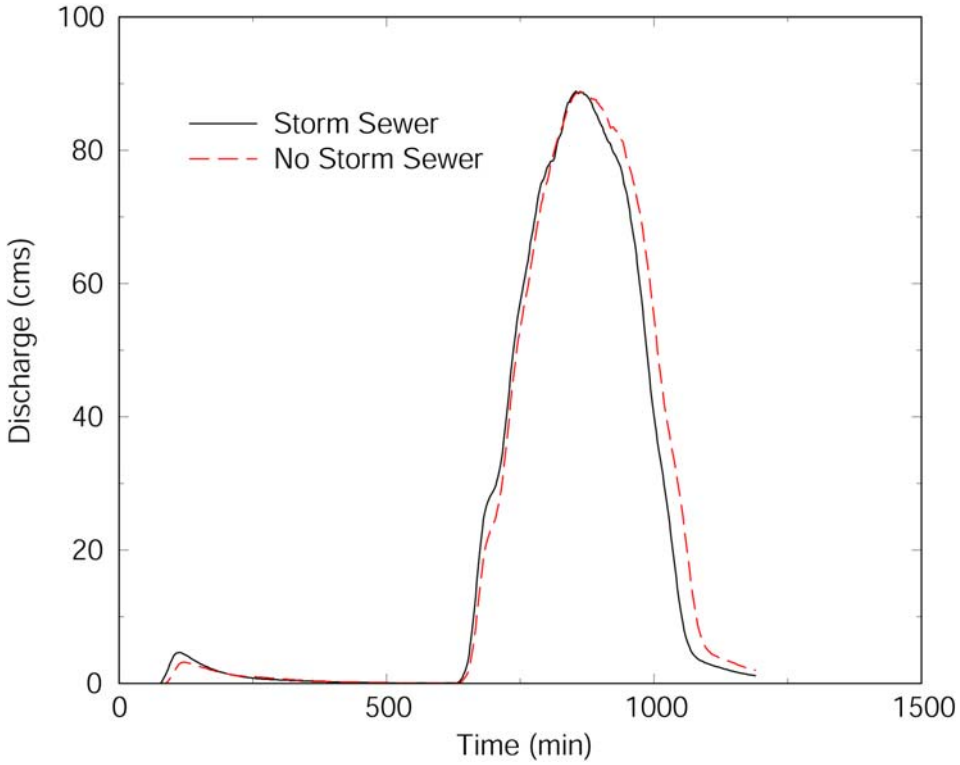

Figure 23 *Reduced effect of storm sewers with extreme event*

Imperviousness

With the drainage network fully functional, it is possible to explore the relative effect of various model components. To assess the question of impervious coverage versus storm drainage, Figure 24 contains plots of sequentially added impervious areas and storm sewers. *Case 1:* no impervious areas, no storm sewer; *Case 2*: distributed impervious areas, no storm sewer; *Case 3*: distributed impervious areas with storm sewer network. All cases include the same channel network, detention basins, and culverts.

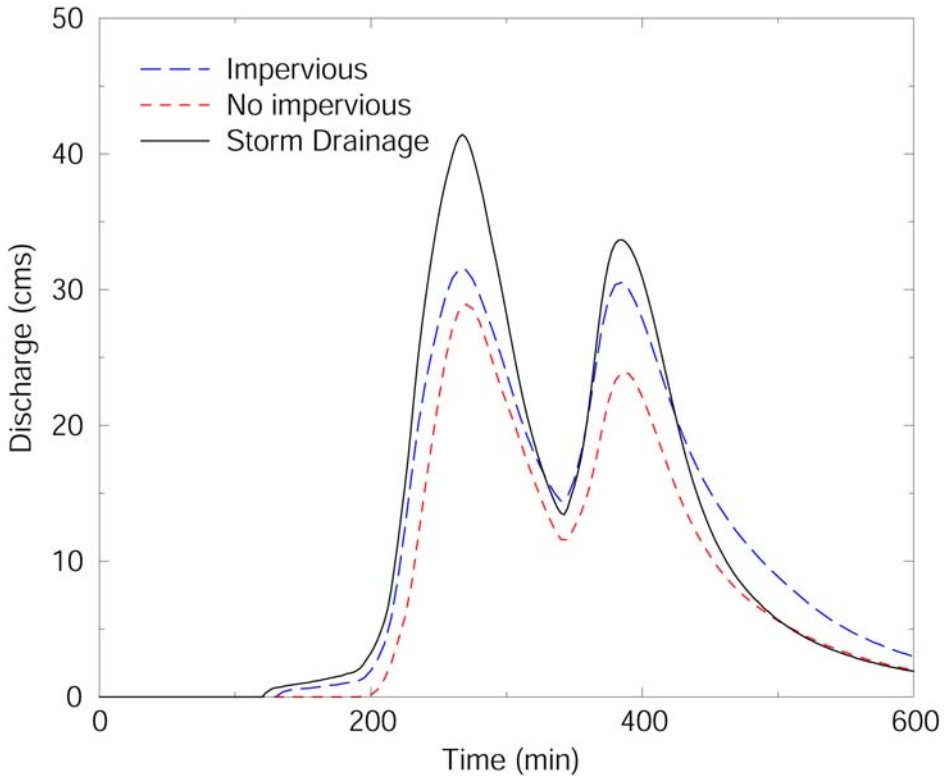

Figure 24 *Comparing effect of imperviousness vs. storm drainage*

Flood magnitudes are amplified by the addition of both impervious coverage and the storm drainage network. The first peak increased 9.1% from Case 1 to Case 2, and 44% from Case 1 to Case 3. This demonstrates the ability of the storm sewers to

drastically alter the peak flood hydrograph. The second peak does not react as much to the addition of storm drains. This can be attributed to the previous discussion of the second pulse's precipitation intensity, which inundated the system. Differences in increase of discharge volume are not as pronounced. From Case 1 to Cases 2 and 3, the increases were 31% and 39% respectively. From this observation, the storm drainage network does not increase discharge volume significantly compared to impervious coverage.

Table 3 Results from modified drainage network simulations

Scenario	*Peak Discharge (cms)*	*Time to Peak (min)*	*Discharge Volume (m^3)*
No imperviousness	28.7	270	298,000
With imperviousness	31.3	268	391,000
Storm Drainage	41.2	267	416,000

It is difficult to isolate the effects of impervious coverage and storm drainage networks. They are not independent processes, as impervious areas feed subsurface culverts and pipes. Although physically unrealistic, it is possible to model them completely separately. Figure 25 shows these two scenarios: *Case 1*: An unsewered watershed with distributed impervious coverage (isolates storm drainage); *Case 2*: A completely pervious watershed with the storm sewer network (isolates imperviousness).

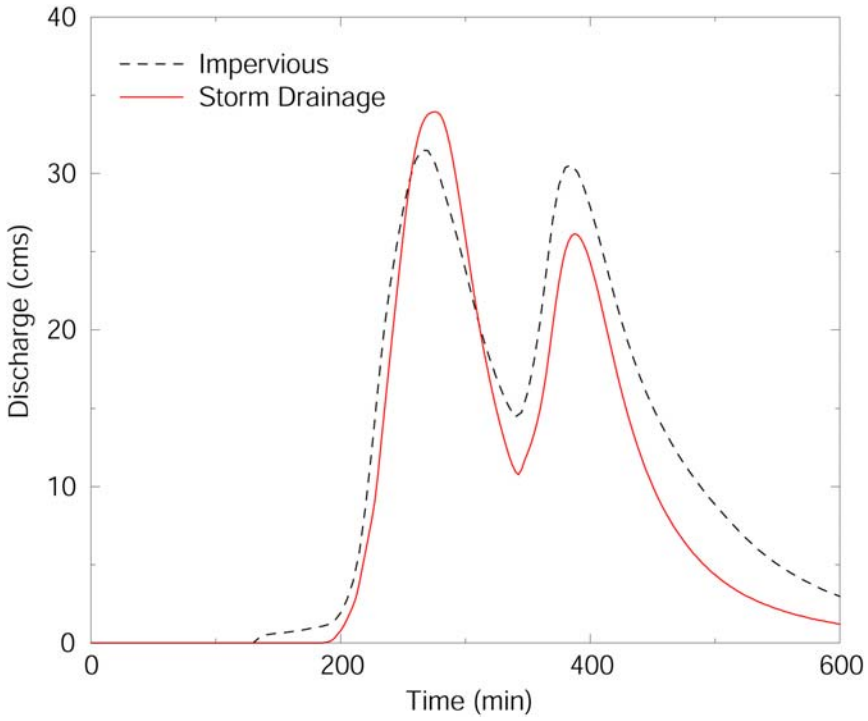

Figure 25 *Isolated effect of storm drainage compared to impervious areas*

The only truly useful observation from this set of simulations occurs at the first peak. Despite the lack of any runoff generating imperviousness in Case 2, the drainage network still produces a higher flood magnitude than Case 1. The fact that imperviousness and the corresponding increased drainage density both play an integral role is not disputed. But by this comparison, it is evident that the drainage network has the capacity to produce a greater effect on flood peaks than imperviousness.

Drainage Density

TOPAZ Networks

Study of the relationship between drainage density and width function required developing a new set of channel networks. While using the existing drainage network would have been preferable, not enough stages of development were available for meaningful analysis. Thus, TOPAZ was once again employed to generate 6 increasingly dense networks, as shown in Figure 26 (a)-(f). To explore the full range of densities, channels were generated by 3.0 km^2 to 0.02 km^2 accumulation thresholds. Comparing Figure 26(a) to Figure 16 shows that this set of networks begins even less dense than the "natural" network used for previous simulations.

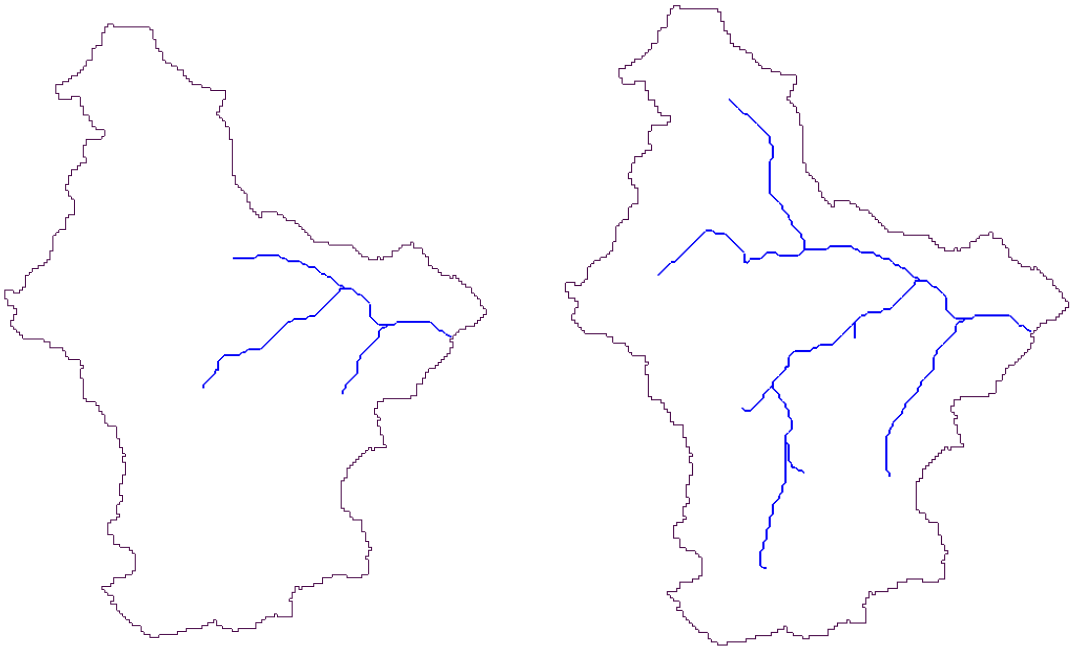

(a) D_d *=0.39 km/km*^{2} *,* A_a *=3.00 km*^{2}

(b) D_d *=0.94 km/km*^{2} *,* A_a *=0.50 km*^{2}

Figure 26 *Increasingly dense drainage networks*
D_d =length of channel / watershed area
A_a =accumulation threshold

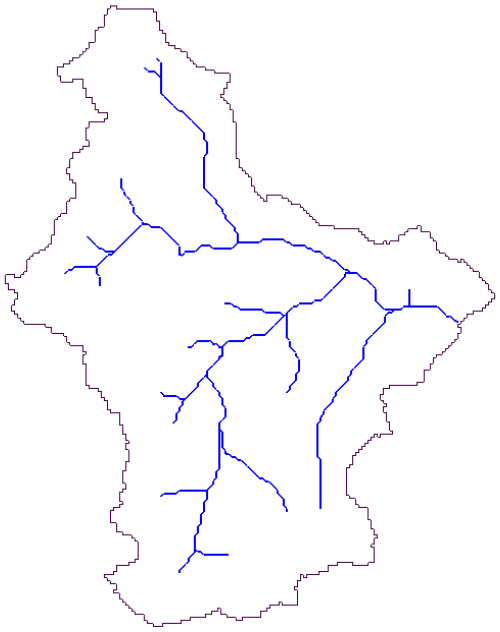

(c) D_d = 1.5 km/km^2
A_a = 0.20 km^2

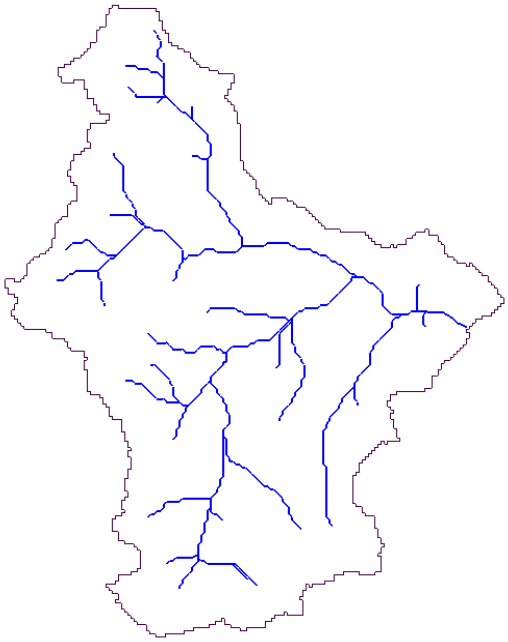

(d) D_d = 2.0 km/km^2
A_a = 0.10 km^2

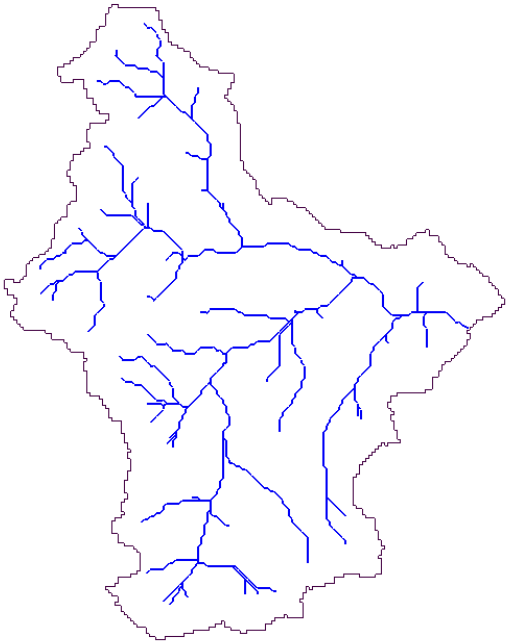

(e) D_d = 2.8 km/km^2
A_a = 0.05 km^2

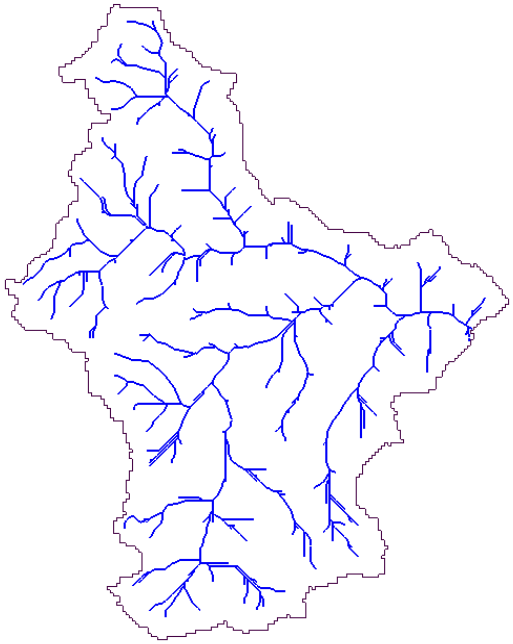

(f) D_d = 4.9 km/km^2
A_a = 0.02 km^2

Figure 26 (cont)

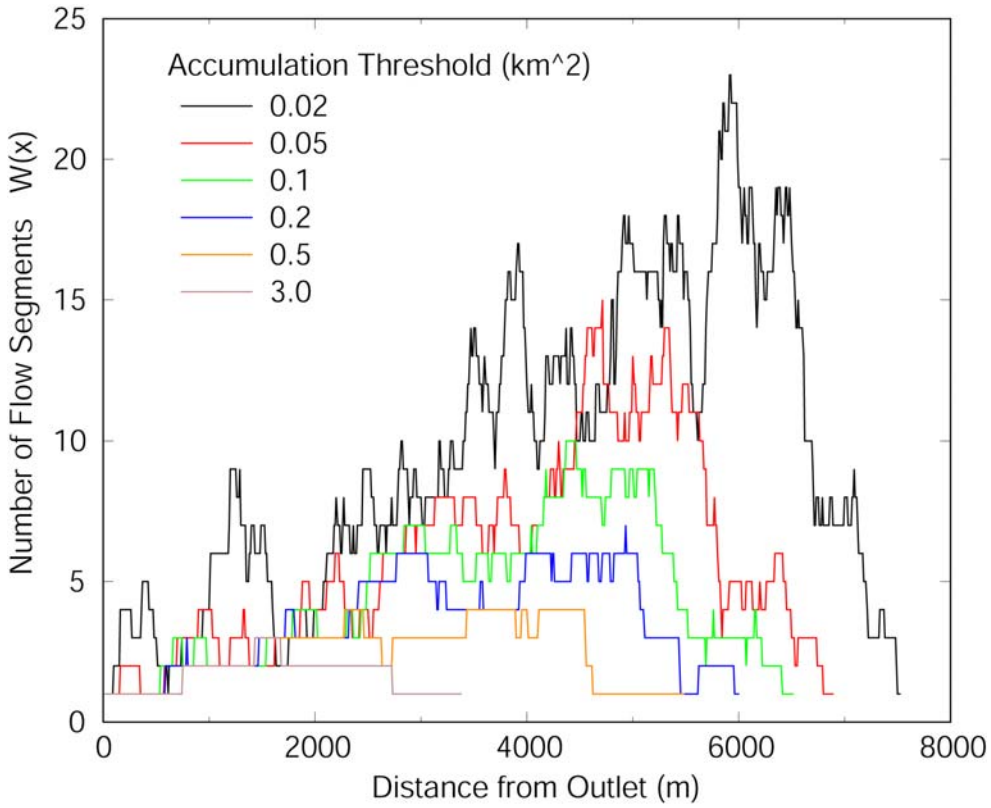

Figure 27 *Equally weighted width functions for 6 networks without storm sewers*

The most valuable observation from the width function plot concerns the proximity of channels to the outlet. Drainage density increases by adding additional channels to the network. Given the shape of the Dead Run watershed, these new channels occur increasingly farther from the outlet. In other words, the central core of the watershed is already almost completely drained, and few links are added in this portion. Thus the distribution of flow segments becomes more and more negatively skewed. The critical statistical measure of the width function is the distance to the mean. This will provide a scalar term describing how far from the outlet most flow segments occur. From visual inspection, a less dense network is expected to have a smaller mean than a very dense network.

Drainage Density Simulations

Determining the effect of both network density and mean width function requires a GSSHA simulation for each test case. These were conducted with identical distributed landuse (with impervious areas), roughness values, and no storm sewers. The channel sizes were kept equal from one network to the next to eliminate the influence of conveyance differences.

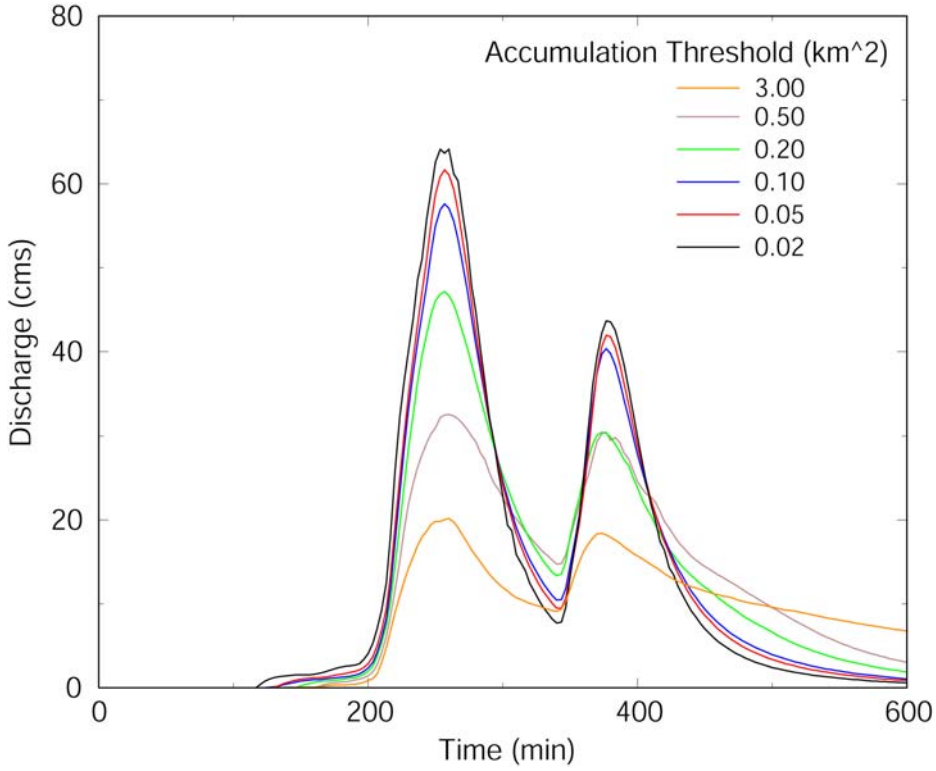

Figure 28 *GSSHA simulation hydrographs for each drainage density, no storm sewers*

Table 4 Results from density simulations

Accumulation Area (km^2)	*Drainage Density D_d (km/km^2)*	*Distance to W(x) Mean (m)*	*Peak Discharge (cms)*	*Time to Peak (min)*	*Discharge Volume (m^3)*
0.02	4.9	4464	65.0	257	445,000
0.05	2.8	4048	61.6	257	443,000
0.10	2.0	3716	57.6	257	437,000
0.20	1.5	3353	47.1	256	418,000
0.50	0.94	2867	32.6	259	399,000
3.00	0.39	1714	20.2	259	285,000

Drainage density clearly has a strong effect on peak discharge, as well as a minor impact on overall volume. The following figure displays both peak discharge and volume from each of the six density scenarios. The drainage density term has units of kilometers of channel per sq km of watershed.

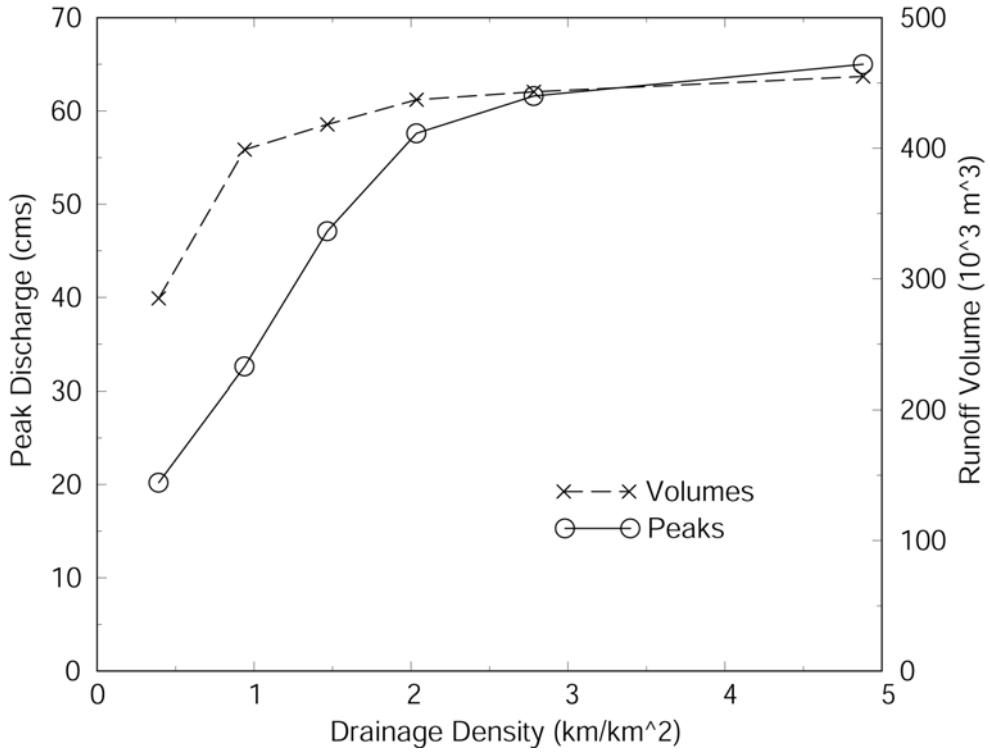

Figure 29 *Effect of channel density on flood peaks*

There is a period of rapid increase from 0.5 to 2 km/km^2, but then levels off beyond 3 km/km^2 where overland flow lengths converge. For this particular watershed, the range of drainage density values to which flood peaks are very sensitive lies less than 2 km/km^2. Beyond this range, additional density does not influence flood peaks as strongly. It appears that that flood peaks are less affected by drainage network expansion once developed past a critical density. This could be particularly significant for a suburban watershed without major modifications to the natural network. If its drainage density were still on the lower end of the sensitive range, relatively minor development could significantly increase flood magnitudes.

Volumetric effects from channel density are not as pronounced (Figure 29). Although densities below 1 km/km^2 display a considerable decrease in discharge, inspection of the hydrograph (Figure 28) shows flow rates well above the other densities. Since a 600 minute simulation time did not allow for complete draining of the watershed at these very low densities, conclusions should not be drawn from them. For the more reasonable densities above 1 km/km^2, runoff volume increases only slightly. As the drainage network expands and becomes more efficient at intercepting overland flow and transporting it to the outlet, there is reduced infiltration opportunity. This volume becomes part of the heightened flood peak as seen in Figure 28.

Width Function

Uniform Density Distribution

As previously defined, distance to the width function mean is a description of spatial distribution of links. The TOPAZ generated networks used throughout this analysis were generated based on contributing area, and this inherently produces uniform density across the entire watershed.

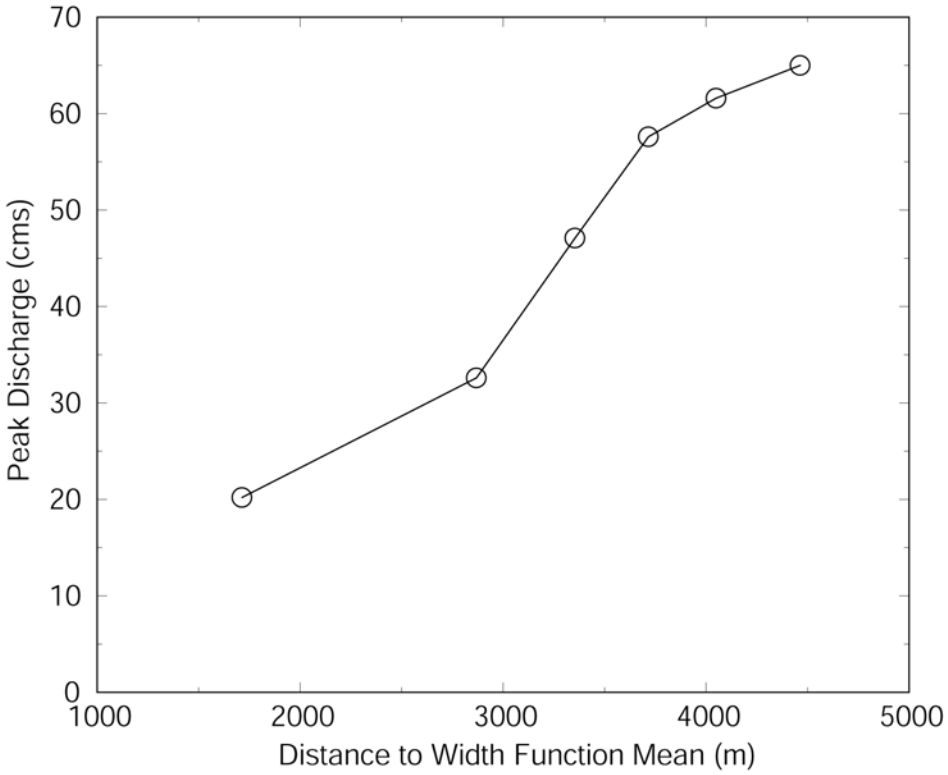

Figure 30 *Effect of proximity of flow segments to outlet on flood peaks*

At first glance, Figure 30 appears to prove that flood peaks increase as the mass of flow arcs move away from the catchment outlet. However, increasing density uniformly over the basin forces the width function mean to move further out. Therefore, the increase in

flood peaks is due to the drainage density, and not the mean distance. Conclusions about the effect of spatial distribution of links cannot be drawn from these simulations.

Distributed Drainage Density

Two scenarios with identical drainage density must be considered to fully explore the effect of non-uniform development within a catchment. Beginning with the densest case (Figure 26 f), channels were removed from either the outer or central regions of the watershed. Selecting certain regions to remain dense produced these two cases (Figure 31). With the drainage density D_d equal in both cases, the effect of spatial variability is simulated without a density bias.

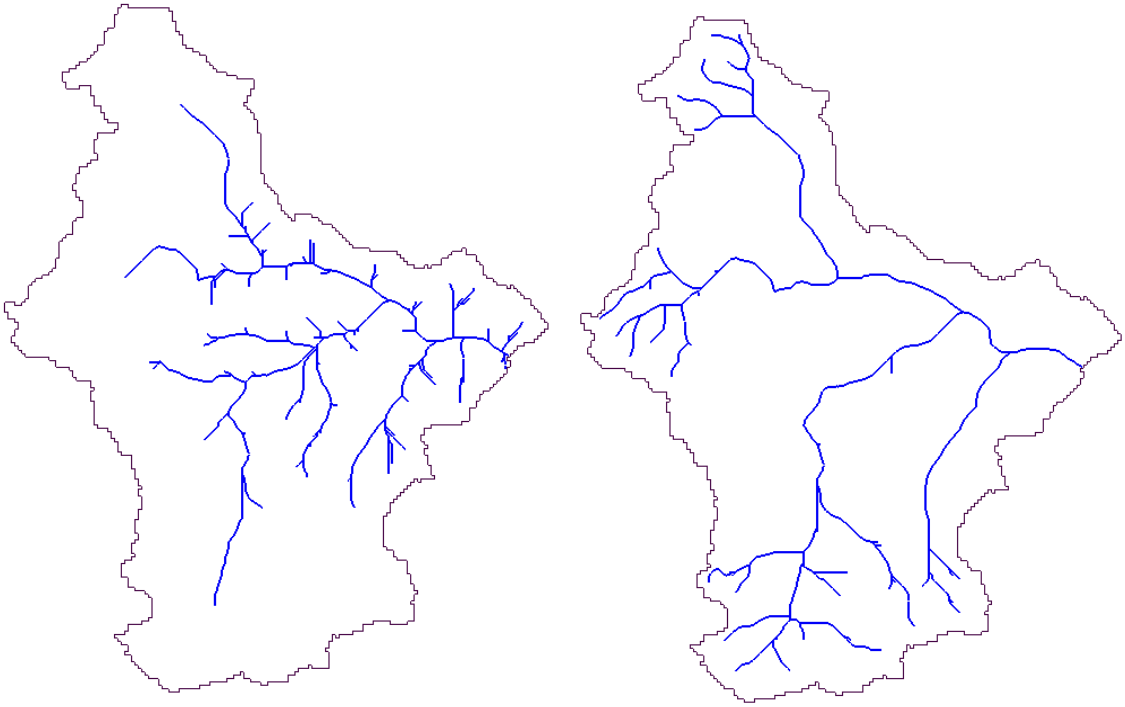

(a) D_d = 2.1 km/km^2 (b) D_d = 2.1 km/km^2

Figure 31 *Spatial extremes of density distribution*

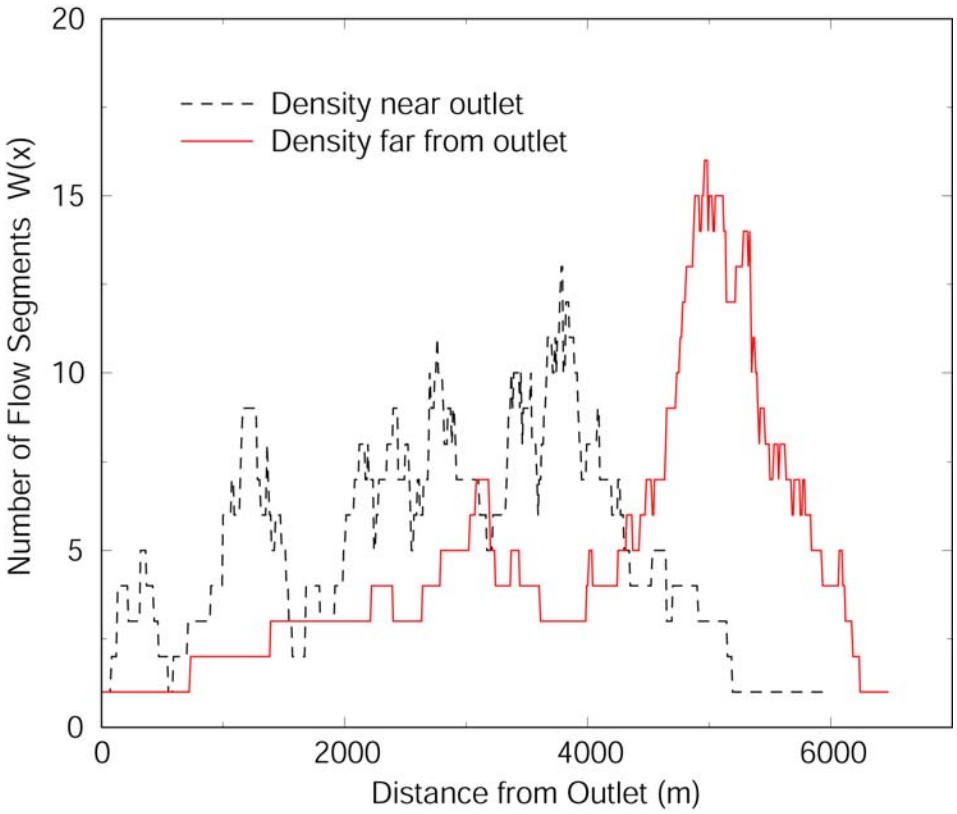

Figure 32 *Width function plots from spatial extremes*

The width functions displayed in Figure 32 appear as expected, as each scenario dominates a portion of the plot based on proximity to the outlet. It is clear from this that identical densities can produce very different mean distances. The normal distribution for density close to the outlet has a mean of 2864 m, but the highly skewed distribution for density far from the outlet yields a mean of 4043 m. Given the drastic differences in mean width function, a significant impact on the hydrology and outlet hydrograph would be expected.

The simulations displayed in Figure 33 contradict this hypothesis. In fact, the first peak is virtually unaffected by the radical change in the drainage network. Although the second peak does exhibit a faster rise and slightly higher peak, the effect is much less

than anticipated. Less travel time in the channel for the case of density close to the outlet allows runoff from the intense second pulse of rainfall to reach the outlet quicker, but substantial volume effects are not evident. The conclusions from these results are simple: distribution of development within this particular watershed does not seem to have a pronounced effect of flood magnitudes, and closer drainage densities to the outlet can slightly reduce the time to peak. It must be noted that the realitely small size of the Dead Run watershed may be critical to this conclusion. Large watersheds in which channel travel time plays a larger role may show very different response to spatial distribution of drainage.

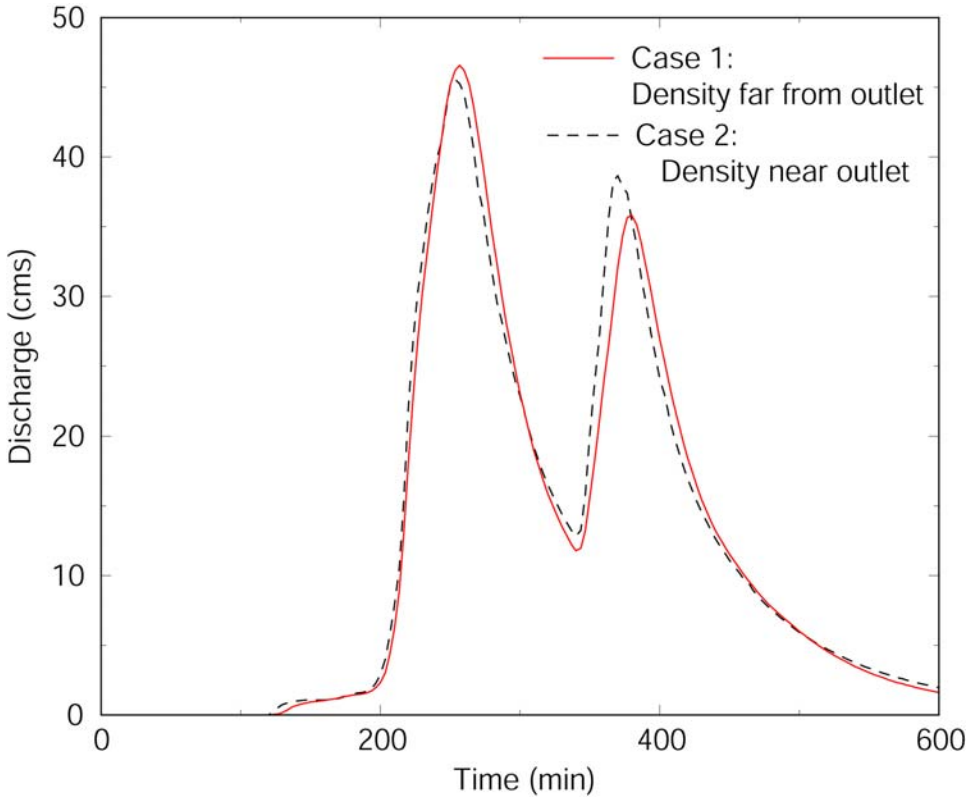

Figure 33 *Effect of density spatial distribution on watershed with impervious areas*

Running identical simulations on a watershed without any impervious coverage tested the influence of impervious area. Thus four cases exist: Case 1: Density far from outlet, with impervious areas, Case 2: Density near the outlet, with impervious areas, Case 3: Density far from outlet, without impervious areas, Case 4: Density near outlet, without impervious areas.

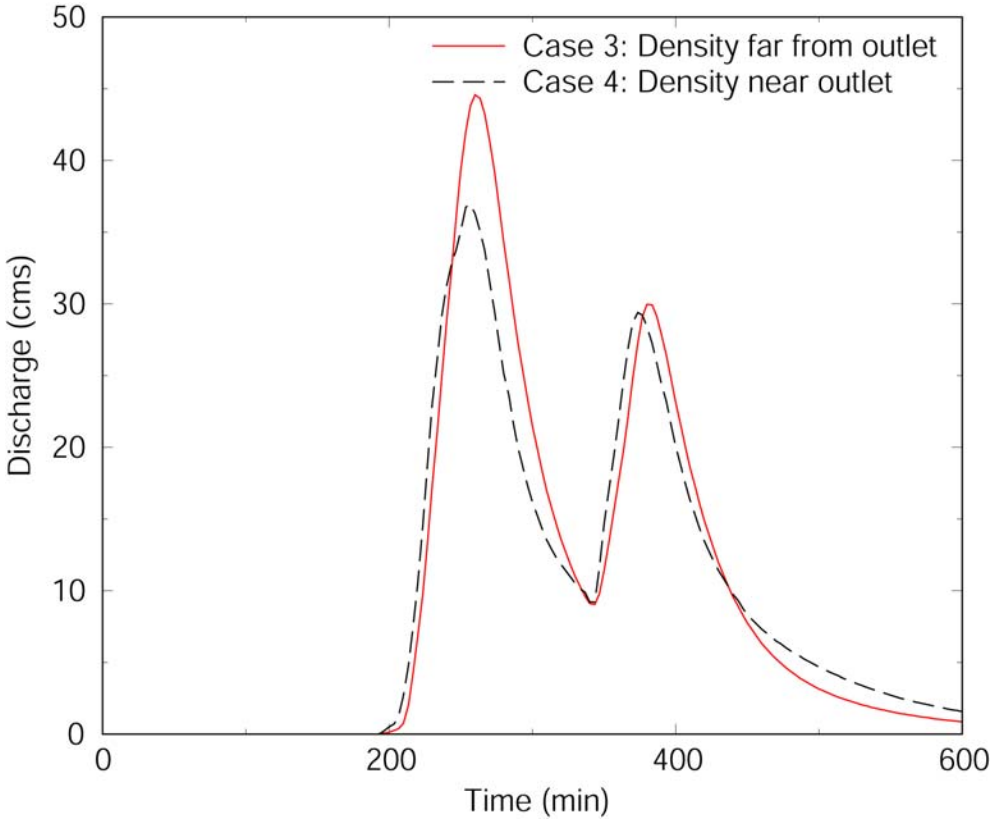

Figure 34 *Effect of density spatial distribution on watershed without impervious areas*

Comparing Figures 33 and 34 demonstrates that distributed impervious area reduces the effect of spatially varied drainage density. For the Cases 3 & 4, without impervious area, significant differences are evident between the two density variations, whereas little contrast was apparent in the Cases 1 & 2. Since much of the impervious area is located at the extremes of the catchment, streets and parking lots in Case 2 could

be reducing overland flow times, enabling a close match to Case 1. For the Cases 2 & 4, with density near the outlet, the decreases in lag time are approximately equal. But peaks, especially the first, are sharply increased by moving the drainage density farther from the outlet in Case 3. Shorter average overland flow lengths will allow less infiltration, thus increasing the total volume of discharge. The increased channel travel length, however, slightly delays this increased flood peak.

Storm Drainage to Accumulation Comparison

Because of the lack of storm sewer modules in many current distributed physically based models, subterranean drainage pipes are often approximated by open channels. By comparing the densest TOPAZ network (Figure 35 b) to the existing Dead Run network with storm drainage (Figure 35 a), the validity of this approximation can be tested.

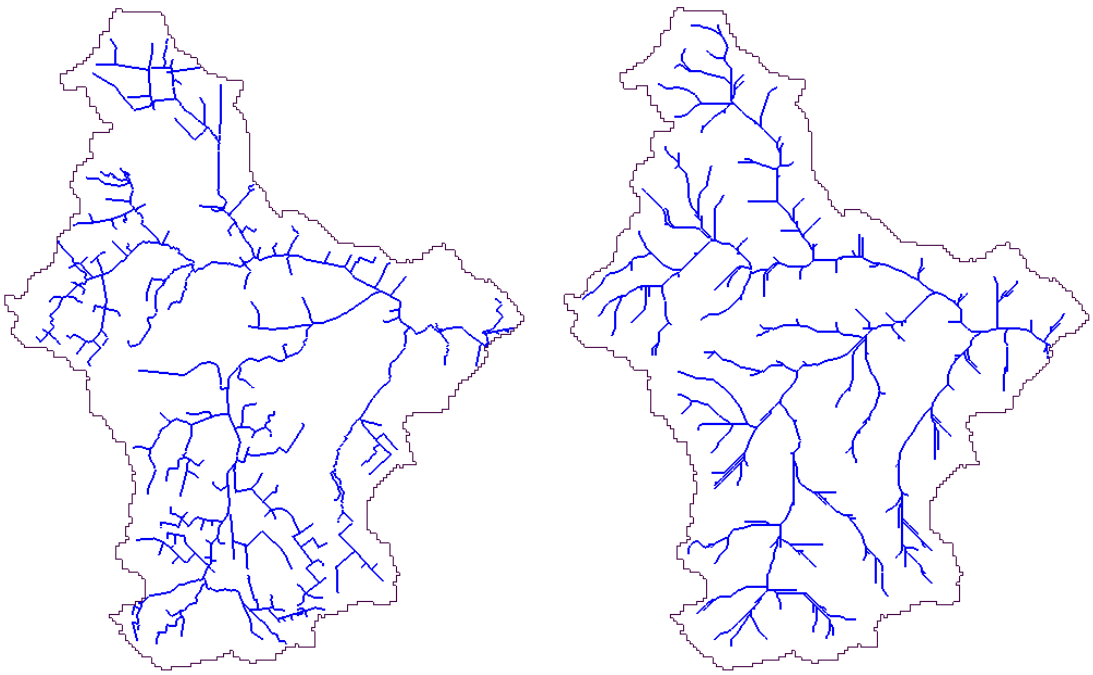

(a) D_d = 5.5 km/km^2 (b) D_d = 4.9 km/km^2

Figure 35 *Drainage network to flow accumulation comparison*

The drainage density D_d = 5.5 km/km^2 for the existing storm drainage network is appreciably more dense than the 0.02 km^2 accumulation threshold network. Figure 36 exhibits the similarities of the two width functions. The distance to the mean width function is likewise greater for the existing system, at 5098 m versus 4464 m. By the preceding arguments, it would follow that the existing system should produce higher peaks.

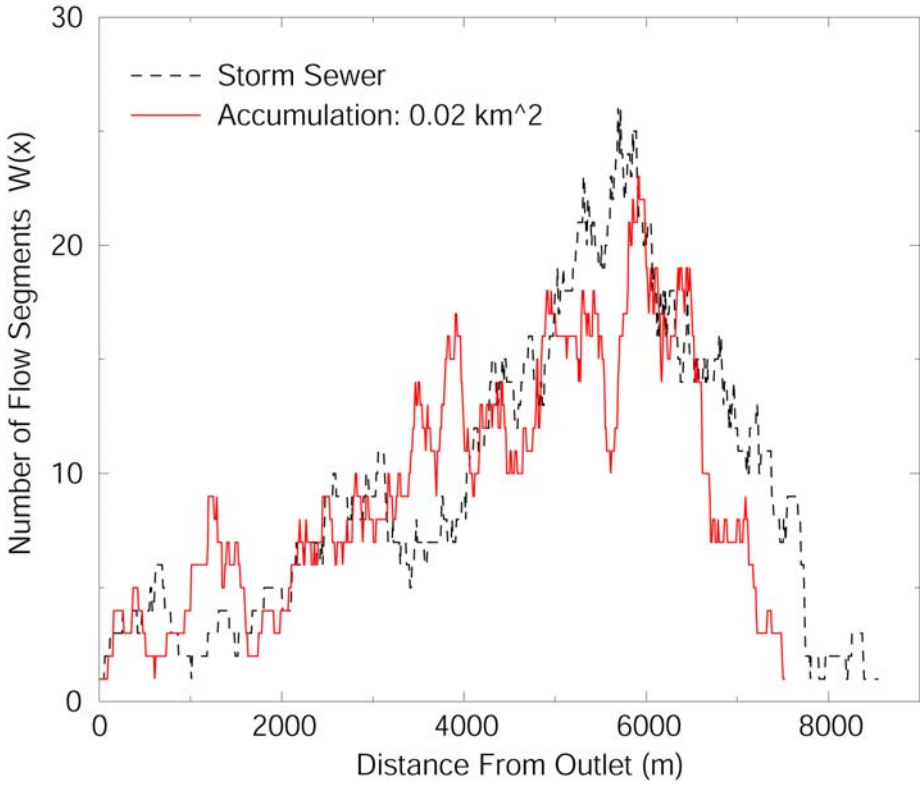

Figure 36 *Width function of drainage network compared to flow accumulations*

However, the channelized network resulted in flood peaks over 65 cms, whereas the existing network simulation produced merely 41 cms at its peak. This disparity in peak flow values is evidence of the profound differences between natural open channels and subterranean pipes. The explanation of this dissimilarity comes in two parts. First, lateral inflow is accepted along the entire length of an open channel but limited to inlet grates for a storm sewer. Second, conveyance in a pipe is far less than even a small open channel because a pipe's enclosed geometry limits high flows. It is clear through the flood magnitude discrepancies that modeling storm sewers with open channels is generally not a sound approximation.

Initial Soil Moisture

Testing the hypothesis that antecedent soil moisture has a significant impact on flood response was performed on both distributed impervious land use and non impervious land use. Simulations results with initial soil degree of saturations of 20%, 60%, and 100% are shown in Figures 37 & 38.

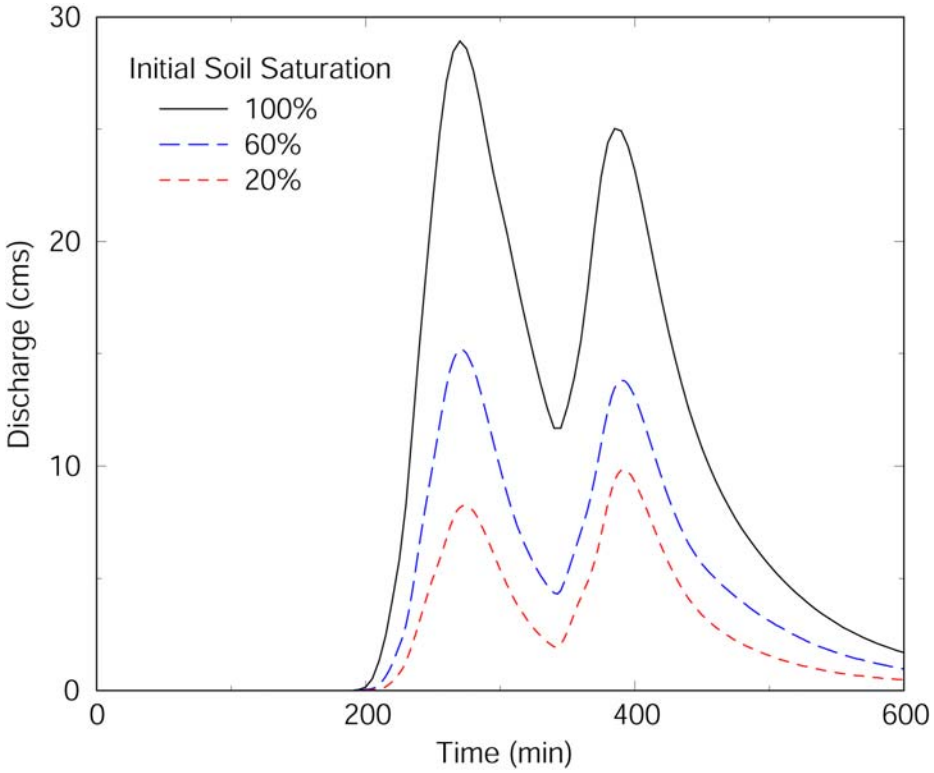

Figure 37 *Effect of antecedent moisture on watershed without impervious area*

The effect of initial soil moisture is clear. It is expected that the effect would be greater in a watershed without impervious area because of the greater influence of soil properties (such as infiltration) in such a basin. But even in the simulation with impervious areas, peaks increased over 40%. Inspection of the peaks in Figures 37 and

38 show that the difference between the peaks of the two scenarios lessens as the initial conditions approach saturation (100%). A fully saturated watershed without impervious area begins to behave much like one with impervious area, but the volume removed by infiltration still decreases peak flows.

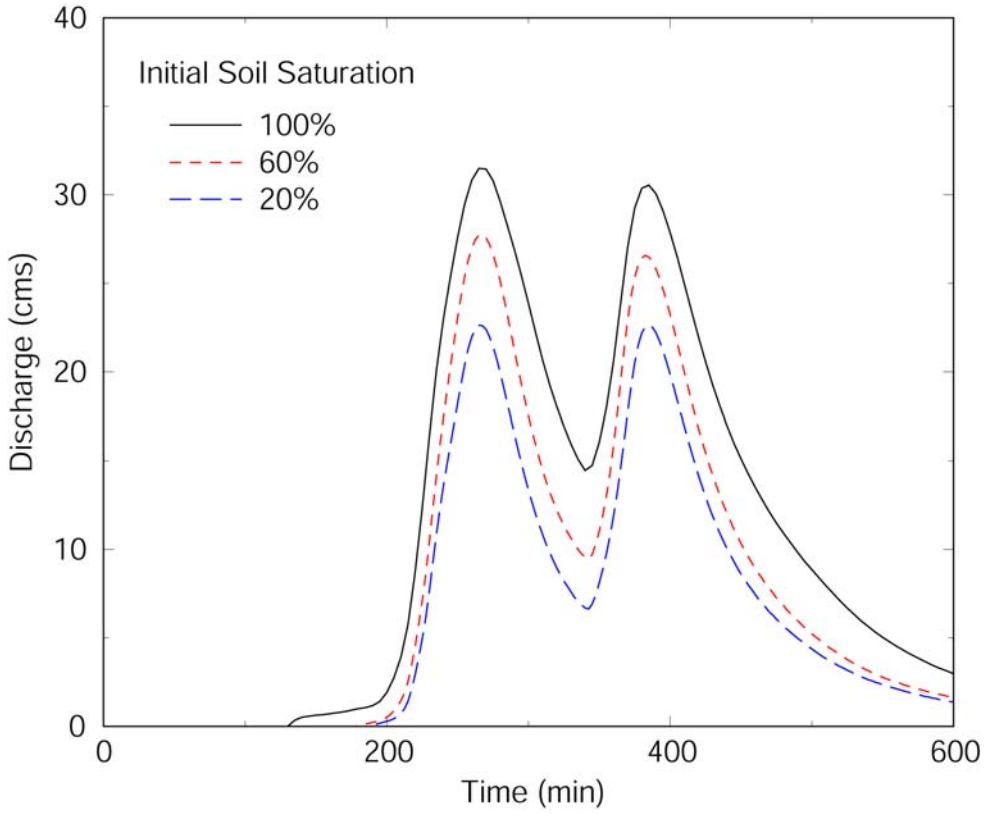

Figure 38 *Effect of antecedent moisture on distributed watershed with impervious areas*

The effect of antecedent moisture is very pronounced for this storm because infiltration still plays a significant role. However, the influence of initial soil saturation is expected to decrease as the intensity of the storm increases. To test this hypothesis, the same Fort Collins extreme event used in the storm sewer section was simulated on Dead Run. The effect of initial soil saturation was greatly reduced, as the saturated test case produced a peak within 5% of the driest case.

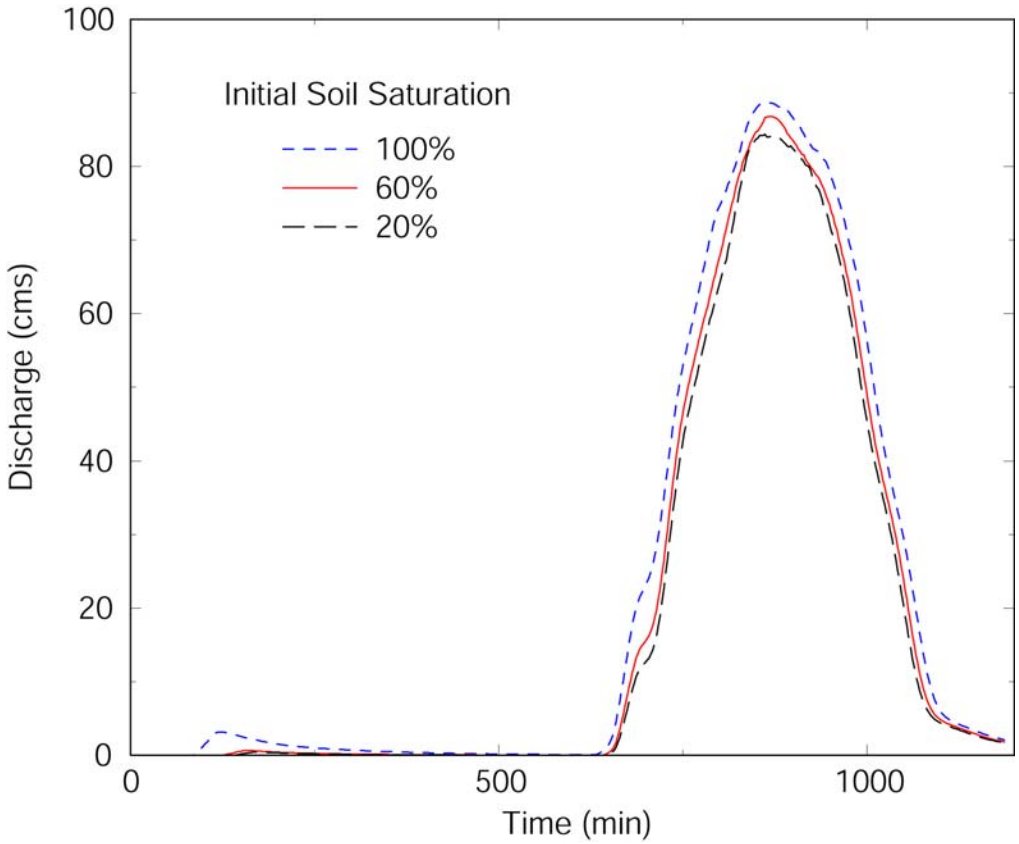

Figure 39 *Minimal influence of antecedent moisture for extreme event*

VI. SUMMARY

Conclusions

Referring to the six key objectives set forth in the thesis introduction, the corresponding conclusions are as follows:

1) A storm drainage model was developed based on an existing algorithm. It was tested for accuracy under a number of scenarios, including reverse flow, backwater effects, and looped networks. This model was then linked to an existing distributed hydrologic model to produce a robust combination capable of simulating the complexities of an urban watershed. Storm sewers should not be modeled as open channels, since they allow too much lateral inflow and do represent realistic intake structures or conveyance properties.
2) Subsurface storm drainage networks have a significant impact on flood peaks for moderate intensity storms. Their relative importance is reduced, however, as rainfall intensity increases and runoff overwhelms the intake structures. For moderate storms, storm sewers were shown to increase peaks by 30%. For extreme events, the influence of storm sewers on flood magnitude disappears.
3) Impervious areas play an important role in the timing of flood peaks. The reduction in surface roughness associated with parking lots and roadways reduces the time to peak of moderate storms. However, for this set of simulations, the relative effect of impervious areas on flood magnitude is less than that of the total storm drainage network.
4) Increasing drainage density has a strong effect on flood peaks, but no influence on flood timing. There is a range of density values to which flood peaks are very

sensitive. Above this range, the network's effect on peaks levels out. Therefore, for a given watershed of some set landuse and rainfall event, the flood magnitude approaches an upper limit.

5) The width function of a channel network with uniform drainage density does not provide an indication of hydrologic response. For non-uniform spatial distribution, the width function was shown to have little effect on flood peaks for small basins. Drainage distribution closer to the outlet slightly reduces the time to peak discharge. Conveyance of open channel networks far surpass closed conduit links, and thus the width function of subsurface flow segments should take into consideration segment geometry.
6) Antecedent soil moisture plays a very important role in flood peaks for moderate intensity events. However, its effect diminishes as an extreme storm's precipitation intensity dwarfs the basin's infiltration capacity.

Engineering Recommendations

Conclusions from this research should not be blindly used as guidelines for development purposes. It is important to note that these findings pertain to small basins of similar geology and soil characteristics. However, it is possible to make some generalized recommendations from this modeling experience. The dominant cause of flooding has been shown to be the ability of a watershed to quickly drain its infiltration excess. This leads to two primary suggestions regarding infiltration and drainage network properties.

It is common to install efficient drainage such as subsurface concrete pipes and straight, clean open channels to alleviate localized flooding problems. This process simply compounds flood magnitudes downstream. Increasing channel roughness through natural means would have a significant impact on attenuating flows. This is possible through the use of shallow, wide, sinuous, grassy swales. Increasing the storage capacity of these "natural" channels could likewise slow discharge.

Increasing the overall quantity of infiltration would decrease the volumes that the channels must ultimately handle. The effect of impervious areas and compacted soils typically found in an urban setting must be mitigated by engineered infiltration devices. These might include subsurface storage cavities that slowly release their content after the storm, as well as converting lawn areas to naturally rough land use such as woodland. It is important to realize that modifications to the natural system have caused the increase in peak discharge, and that re-introducing these natural mechanisms a way to reverse the trend of urban flooding.

Future Research

The research conducted throughout this thesis spawned a number of ideas for future studies. A number of these suggestions relate to the data of Dead Run and Hurricane Isabel. It would be valuable to model the watershed with a finer 10 meter DEM to determine if the losses from aggregation were negligible. Improving the detail of the sub-surface drainage network could provide further analysis of its influence. As discussed in the model results section, the single radar bias value did not accurately represent the second pulse of rainfall. Different bias values could be applied to the two storm pulses, while still conserving storm total rainfall. Similarly, time series rain gage data could be compared to the radar results. These improvements of model input would enable a better match of the simulated and observed outlet hydrographs.

Further investigation on the impact of impervious areas on flood timing would provide valuable conclusions. The approach might be to vary the percent of impervious area as well as its distribution within the watershed in the same manner as the drainage density trials were executed.

Additional research could focus on comparing multiple watersheds and their drainage densities. By comparing the upper threshold of flood magnitude found in this thesis to that of other basins, one could determine whether the drainage density values are transferable.

VII. WORKS CITED

Anderson, D. G., 1970: *Effects of urban development on floods in northern Virginia*. U.S. Geological Survey Water Supply Paper 2001-C, 22pp.

Beighley, R.E., and G.E. Moglen, 2003: Adjusting measured peak discharges from an urbanizing watershed to reflect a stationary land use signal. *Water Resour. Res.*, **39**, WES 4-1 – WES 4-11.

Chow, V.T., D.R.Maidment, L.W. Mays, 1988: *Applied Hydrology.* McGraw-Hill, Inc.

Crooks, S. and H. Davies, 2001: Assessment of land use change in the Thames catchment and its effect on the flood regime of the river. *Phys. Chem. Earth*, **26** (7-8), 583-591.

Downer, C.W., and F.L. Ogden, 2004, GSSHA: A model for simulating diverse streamflow generating processes, *J. Hydrol. Engrg.*, 9(3):161-174.

Garbrecht, J., and L.M. Martz, 1993, "Case application of the automated extraction of drainage network and subwatershed characteristics from digital elevation models by DEDNM," AWRA Proceedings of the Geographic Information Systems and Water Resources, March 1993, pp. 221-229.

Graf, W.L., 1977: Network characteristics in suburbanizing streams. *Water Resour. Res.*, **13**, 459-463.

Howe, J. and I. White, 200X: Flooding: Are we ignoring the real problem and solution? *Policy Review Section*, 368-370.

Hsu, M.H., S.H. Chen, T.J.Chang, 2000: Inundation simulation for urban drainage basin with storm sewer system. *J. Hydrology*, **234**, 21-37.

Ji, Zhong, 1998: General hydrodynamic model for sewer/channel network systems. *J. Hydraulic Eng.*, **124**, 307-315.

Leopold, L.B., 1968: *Hydrology for urban planning- a guidebook on the hydrologic effects of urban land use*: U.S. Geological Survey Circular 554, 18 pp.

Mays, L.W., 1999: *Hydraulic Design Handbook*, McGraw-Hill, Inc.

Morrison, J.E., J.A. Smith, 2002: Stochastic modeling of flood peaks using the generalized extreme value distribution. *Water Resour. Res.* **38-12**, 41-1 – 41-12.

Ogden, F.L., H.O. Sharif, S.U.S. Senarath, J.A. Smith, M.L. Baeck, and J.R. Richardson, 2000, Hydrologic Analysis of the Fort Collins, Colorado, Flash Flood of 1997, *J. Hydrology*, 228, pp. 82-100.

Reynard, N.S., C. Prudhomme, S.M. Crooks, 2001: The flood characteristics of large U.K. rivers: Potential effects of changing climate and land use. *Climatic Change*, **48**, 343-359.

Richards-Pecou, B., 2002: Scale invariance analysis of channel network width function and possible implications for flood behaviour. *Hydrological Sci.-J.,* **47**, 387-404.

Rodriguez-Iturbe, I., and A. Rinaldo, 1997: *Fractal River Basins*. Cambridge University Press, 547 pp.

Smith, J.A., J.E. Morrison, P. Sturdevant-Rees, D.F. Turner-Gillespie, P.D. Bates, 2002: The regional hydrology of extreme floods in an urbanizing drainage basin. *J. Hydromet.*, **3**, 267-282.

Troch, P.A., J.A. Smith, E.F. Wood, F.P. de Troch, 1994: Hydrologic controls of large floods in a small basin: central Appalachian case study. *J. Hydrology*, **156**, 285-309.

Turner-Gillespie, D.F., J.A. Smith, P.D. Bates, 2003: Attenuating reaches and the regional flood response of an urbanizing drainage basin. *Adv. Water Resour.,* **26**, 673-684.

Valeo, C., Moin, S.M.A., 2001: Hortonian and variable source area modeling in urbanizing basins. *J. Hydrologic Eng.,* July/August 328-335.

Veitzer, S.A., and V.K. Gupta, 2001: Statistical self-similarity of width function maxima with implications to floods. *Adv. Water Resour.*, **24**, 955-965.

Wolff, G.C. and S.J. Burges, 1994: An analysis of the influence of river channel properties on flood frequency. *J. Hydrology*, **153**, 317-337.

VIII. APPENDICES

APPENDIX A

GSSHA & SUPERLINK Link Process

The combined GSSHA and SUPERLINK codes will operate in the following manner:

1) Initial drainage network setup
    a. GSSHA reads coordinates of all manholes, grates, and junctions from the SUPERLINK input file
    b. GSSHA determines the cell index for each manhole, grate, and junction
    c. GSSHA reads the channel node/link index for each downstream junction emptying into a channel
2) GSSHA calls SUPERLINK
    a. GSSHA passes the water surface elevation at each junction, whether in a channel or on the overland flow plain
    b. GSSHA passes the depth of water in each cell containing a grate
3) SUPERLINK is executed
    a. SUPERLINK sets boundary conditions for all downstream junctions with associated water surface elevations
    b. SUPERLINK determines the depth of water at each grate
    c. If the head at a grate is less than the ground surface elevation, SUPERLINK inserts all flow into the grate
    d. SUPERLINK searches for any grate, manhole, or junction heads greater than the ground surface elevation and calculates the excess to return to the overland plain
    e. SUPERLINK runs one timestep
4) SUPERLINK returns values to GSSHA
    a. SUPERLINK passes the amount of water taken from or added to an overland cell
    b. SUPERLINK passes the discharge from downstream junctions to a channel node/link or overland flow cell

APPENDIX B

SUPERLINK Input File

The assimilation of these three separate files required a separate piece of code. This simple algorithm looped through each superlink, acquiring connectivity information, node positions, and pipe sizes. Quality control was a serious concern at this point, as the volume of manual data entry left ample room for error. Counters were coded into the routine to search for incorrect number of occurrences of junctions. These checks proved invaluable for detecting human blunders. Using the UTM coordinates of each point, the length was calculated for each pipe segment. The output from this program was the format required by SUPERLINK, as can be seen in this sample. Fields represent parameters as defined by the following cards:

```
CONNECT  "SUPERLINK #"  "UPSTREAM JUNCTION"  "DOWNSTREAM JUNCTION"

SJUNC  "JUNCTION #"  "GROUND SURFACE ELEVATION m"  "JUNCTION BOTTOM
       ELEVATION m"  "SURFACE AREA m2"  "INLET CODE"  "UTM NORTHING"
      "UTM   EASTING"

SLINK  "SUPERLINK #"  "NUMBER OF NODES"

NODE  "NODE #"  "GROUND SURFACE ELEVATION m"  "INVERT ELEVATION m"
      "SURFACE AREA m2"  "INLET CODE"  "UTM NORTHING"  "UTM   EASTING"

PIPE  "PIPE #"  "SECTION TYPE"  "DIAMETER m"  "SLOPE"  "ROUGHNESS n"
      "LENGTH m"

CONNECT    1     1     2
SJUNC   1   143.59  139.43  2.000000  1    348491.615300 4354294.986100
SJUNC   2   137.38  136.43  4.000000  999  348759.887900 4354212.379000
SLINK   1   11
NODE  1   143.59   139.43  0.000000  777  348491.615300  4354294.986100
NODE  2   141.73   139.04  1.000000    2  348528.220900  4354281.109000
NODE  3   143.94   138.81  0.500000    0  348538.205500  4354261.139800
NODE  4   142.27   138.46  0.500000    0  348572.438500  4354251.868400
NODE  5   141.05   138.17  0.500000    1  348580.996700  4354279.682600
NODE  6   141.90   137.74  1.000000    2  348622.361500  4354268.984800
NODE  7   140.89   137.48  0.500000    0  348613.803300  4354244.023300
NODE  8   140.29   137.03  0.500000    0  348658.020900  4354234.751900
NODE  9   140.29   136.88  0.500000    0  348654.454900  4354220.488200
NODE 10   137.50   136.46  0.500000    1  348705.804400  4354211.216700
NODE 11   137.50   136.45  0.000000  777  348706.517600  4354228.333200
```

```
NODE 12   137.38   136.43  0.000000  777  348759.887900  4354212.379000
PIPE  1  1  0.457200  0.010000  0.012000   39.15
PIPE  2  1  0.457200  0.010000  0.012000   22.33
PIPE  3  1  0.457200  0.010000  0.012000   35.47
PIPE  4  1  0.457200  0.010000  0.012000   29.10
PIPE  5  1  0.457200  0.010000  0.012000   42.73
PIPE  6  1  0.457200  0.010000  0.012000   26.39
PIPE  7  1  0.457200  0.010000  0.012000   45.18
PIPE  8  1  0.457200  0.010000  0.012000   14.70
PIPE  9  1  0.457200  0.008000  0.012000   52.18
PIPE 10  1  0.457200  0.000500  0.012000   17.13
PIPE 11  1  0.457200  0.000500  0.012000   55.70
```